α-tubulin^{4} is essential for the formation of long microtubules to push apart the daughter centrosomes along the nuclear perimeter during early Drosophila embryogenesis

Zsolt Venkei

DOCTOR OF PHILOSOPHY DISSERTATION
IN CELL BIOLOGY

UNIVERSITY OF SZEGED, FACULTY OF MEDICINE,
DEPARTMENT OF BIOLOGY

AND

MATERNAL EFFECT AND EMBRYOGENESIS RESEARCH
GROUP OF THE HUNGARIAN ACADEMY OF SCIENCES

Supervisor: János Szabad

2006

CONTENTS

PUBLICATIONS RELATED TO THE THESIS

- Venkei Zsolt, Gáspár Imre és Szabad János, Pályák és motorok a sejtosztódásban. Természet Világa **6**, 247-250, 2005.

- Venkei, Z. and Szabad, J., The *Kavar*^{D} dominant female-sterile mutations of Drosophila reveal role of the maternally provided α-tubulin^{4} isoform in cleavage spindle maintenance and elongation. Molecular Genetics and Genomics **273**, 283-289, 2005. IF: 2,371

- Venkei, Z., Gáspár, I., Tóth, G. and Szabad, J., α-tubulin^{4} is essential for rapid formation of lengthy interpolar MTs to push apart the daughter centrosomes along the nuclear perimeter during early Drosophila embryogenesis. J Cell Science, 2006, accepted for publication, DOI 03039, IF: 6,910.

ORAL PRESENTATIONS

- Venkei Zsolt, Belecz István és Szabad János, Mi mindent tanultunk a mikrotubulusokról a *Kavar*^{D} mutációk tükrében? V. Magyar Genetikai Kongresszus. Siófok, April 13-15, 2003.

- Venkei Zsolt és Szabad János, Mi mindent tanultunk a mikrotubulusokról a *Kavar*^{D} mutációk tükrében? I. A Magyar Genetikai Intézetek Találkozója, Szeged, September 5, 2003.

- Gáspár Imre, Venkei Zsolt és Szabad János, Hogyan függ a mikrotubulusok hossza az anyai eredetű α-tubulintól? A méret a lényeg? VI. Magyar Genetikai Kongresszus, XIII. Sejt- és Fejlődésbiológiai Napok. Eger, 2005. április 10-12.

- Szabad János, Gáspár Imre és Venkei Zsolt, Miért tesznek a muslica nőstények anyai eredetű α-tubulint petéikbe? VI. Magyar Genetikai Kongresszus, XIII. Sejt- és Fejlődésbiológiai Napok. Eger, Eger, 2005. április 10-12.

- Venkei Zsolt, Gáspár Imre és Szabad János, Mikrotubulusok az osztódási orsóban: váz, pálya és erőkifejtés. VI. Magyar Genetikai Kongresszus, XIII. Sejt- és Fejlődésbiológiai Napok. Eger, Eger, 2005. április 10-12..

- Zsolt Venkei, Imre Gáspár and János Szabad, Drosophila mothers supply the egg cytoplasm with α-tubulin^{4} to ensure the assembly of long MTs. XIX. European Drosophila Research Conference. Eger, August 31- September 3, 2005.

POSTER PRESENTATIONS

- Venkei Zsolt, Szabad János, Mi mindent tanultunk a sejtváz szerveződéséről a Drosophila Kavar mutációjának tükrében? X. Sejt- és Fejlődésbiológiai Napok. Siófok, March 27-29, 2002.

- Zsolt Venkei, Kamill Bálint, Imre Gáspár, Miklós Erdélyi, Jordi Casanova and János Szabad, A dominant female-sterile mutation in the maternal α-tubulin gene of Drosophila reveals novel MT associated functions in egg cytoplasm and in embryogenesis. EMBO/FEBS Workshop: Frontiers in cytoskeleton research, Gosau (Austria), September 13-18, 2003.

- Zsolt Venkei, Imre Gáspár and János Szabad, The maternally provided α-tubulin isoform ensure the assembly of long MTs in early Drosophila embryos. FEBS Course on Advenced Light Microscopy and 5th International Meeting of European Light Microscopy Initiative, Semmerlin (Austria), May 31-June 3, 2005.

- Zsolt Venkei, Imre Gáspár and János Szabad, The maternally provided α-tubulin isoform ensure the assembly of long MTs in early Drosophila embryos. EMBO Practical Course on Microinjection and detection of probes in living cells. Heidelberg (Germany), June 26- July 2, 2005.

ABBREVIATIONS

BRB80	buffer with 80 mM Pipes, 2 mM MgCl2 and 1 mM EGTA
BSA	bovine serum albumin
Df	deficiency
Dm	*Drosophila melanogaster*
DMSO	dimethyl-sulfoxide
Dp	duplication
FITC	fluorescein-isothyanocyte
Fs	dominant female-sterile mutation
GAL4	positive regulator of gene expression for the galactose-induced genes in *Saccharomyces cerevisiae*
GFP	green fluorescent protein
KLP61F	Kinesin-like protein at 61F
kavar^{r}	revertant (loss-of-function) allele of a *Kavar*^{D} dominant female-sterile mutation
MAP	MT-associated protein
MT	microtubule
Ncd	non-claret disjunctional plus-minus kinesin
PBST	isotonic phosphate buffer with NaCl and 0.1 % Tween-20
PCR	polymerase chain reaction
SDS	sodium-dodecyl-sulphate
SDS-PAGE	SDS poly-acrylamide gel electrophoresis
TG	transgene
UAS	upstream activator sequence in *Saccharomyces cerevisiae*

INTRODUCTION

Embryos in the animal kingdom rely largely on maternally provided molecules at the very beginning of their life (DeRenzo and Seydoux, 2004). Mediators of maternal effect are synthesized under control of the maternal genes and are deposited into the egg cell cytoplasm during oogenesis. To identify egg cytoplasm components required for the commencement of embryogenesis we made use of the "genetic dissection" technique: induced and isolated dominant female-sterile (*Fs*) mutations including the $Kavar^{D}$ alleles: $Kavar^{18c}$, $Kavar^{21g}$ and $Kavar^{21l}$ of *Drosophila melanogaster*. The *Fs* mutations allow the formation of normal-looking and fertilized eggs, however embryogenesis can not commence inside the eggs (Erdélyi and Szabad, 1989; Szabad *et al.*, 1989). We anticipated that if an *Fs* mutation prevents the commencement of embryogenesis, product of the *Fs*-identified normal (+) gene is involved in the process and molecular analysis of the normal gene would shed light on the beginning of a new life. We also induced, through second mutagenesis, revertant alleles of the *Fs* mutations and used those in complementation analyses. Allelism of the $Kavar^{D}$ mutations was inferred from the finding that the $kavar^{r}$ revertant alleles do not complement: the $kavar^{r}/kavar^{r}$ females are sterile (Erdélyi and Szabad, 1989). Making use of the dominant negative nature of the $Kavar^{D}$ alleles and sterility of the $kavar^{rl}/-$ hemizygous females we mapped and cloned the gene and learnt that the $Kavar^{D}$ and the $kavar^{r}$ alleles identify the formerly described *α-tubulin 67C* gene which encodes synthesis of α-tubulin[4], the so-called maternal α-tubulin isoform. Expression of the *αtub67C* gene is restricted to the female germ line and the early embryo (Kalfayan and Wensink, 1982; Matthews *et al.*, 1989; Theurkauf, 1992; Matthews *et al.*, 1993; Máthé *et al.,* 1998; Matthies *et al.*, 1999).

α-tubulin (a subunit of the α-β-tubulin heterodimers and the MTs) plays an essential role in all MT dependent processes in the living cells. The MTs are dynamic cytoskeletal structures that function in eukaryotes to segregate chromosomes during cell division, posit cell organelles, organize sell shape (the outgrowth of axons and dendrites) and provide shape and motility to cilia and flagella (reviewed by Downing and Nogales, 1998; Dutcher, 2001; Kwon and Scholey, 2004). An important feature of the MTs is that they are dynamic; at steady state, individual MTs can independently alternate between periods of stability (lengthening) and instability (shrinking or catastrophe; Mitchison and Kirschner, 1984). *In vivo* the rate of polymerization is much higher than expected for the concentration of tubulin in the cytoplasm but is nevertheless also associated with a high rate of catastrophe. Clearly, MT-associated proteins (MAPs) exist *in vivo* which account for the differences and play an important role in modulating the behavior and organization of the MTs (Cassimeris, 1993).

The forces that act in association with the MTs in cellular processes are mainly of two types: (1) pushing and pulling forces at the tips of MTs generated by polymerization and depolymerization of the MTs (Dogterom *et al.*, 2005) and (2) forces generated by ATP-consuming motor protein movement along the MT-tracks (Mallik and Gross, 2004; Kwon, Scholey, 2004; Brust-Mascher et al., 2004). In more complex MT-dependent cellular processes - like in segregation of the daughter centrosomes and sister chromatids - both types of forces act in parallel and in well-coordinated fashion (Cytrynbaum *et al.*, 2003; Moore and Wordeman, 2004).

MTs are composed from α-β-tubulin heterodimers, in which the α- and the β-tubulin proteins - approximately 450 amino acids each - are highly homologous. The overall structure is very similar for the two types of tubulins. Each monomer binds a GTP that is nonexchangeable in α-tubulin and exchangeable in β-tubulin. In the dimmer, the nucleotide in the α-subunit is buried at the intradimer interface explaining its none changeable nature (Figure 1; Lowe *et al*., 2001). The nonexchangeable GTP control structural stability of the tubulin dimer by a high-affinity bound Mg^{2+} (Menendez *et al*., 1998). The exchangeable GTP is required for MT assembly, and its hydrolysis follows addition of a dimer to the MT end, upon which it becomes non-exchangeable (Figure 1; Nogales, 1999).

In living cells a set of α- and β-tubulin variants build up the MTs. The variants (called isotypes) are products of different α- and β-tubulin coding genes. There are up to seven members of both the α- and the β-tubulin gene families in the genome of the animal cells (Kalfayan and Wensink, 1981; Sullivan, 1988; Luduena, 1998). However while both α- and β-tubulin isotypes share high homology, they posses characteristic divergences both in structure and function. They differ most considerably in the C-terminal 15-20 amino acids, in the region that is positioned on the exterior of the MTs. Even slight differences between the amino acid sequences of two isotypes can lead to remarkable differences in the cellular functions (Hutchens *et al*., 1997). Each isotype has a characteristic spatial and temporal expression pattern throughout ontogenesis. Some isotypes are abundantly expressed in a variety of tissues, whereas other isotypes exhibit tissue and developmental stage specific expression (reviewed by Luduena, 1998). Despite their specificity, several studies have demonstrated that tubulin isotypes are *in vitro* and *in vivo* freely interchangeable and co-assemble into all classes of MTs (Lewis *et al*., 1987; Downing and Nogales, 1998). The biochemical properties of the MTs are clearly determined by the incorporated tubulin isotypes. Presence of an α- or a β-isotype can influence length and stability (Bhattacharya and Cabral, 2004), dynamics (Bode *et al*. 2003) or the drug resistance of the MTs (Kamath *et al*.,

2005). It was also demonstrated in the Nematode and the Drosophila model systems, that a given α- or β-tubulin isotype can be essential for one or more MT dependent cellular processes (Dettman *et al*., 2001; Matthews *et al*., 1993; Wright and Hunter, 2003). Whereas all the above listed works demonstrate that the integration of a particular isotype is required for at least one MT dependent process in a studied cell type, the question to ask is this: what sort of modification renders the MTs competent to carry on a well-defined cellular process?

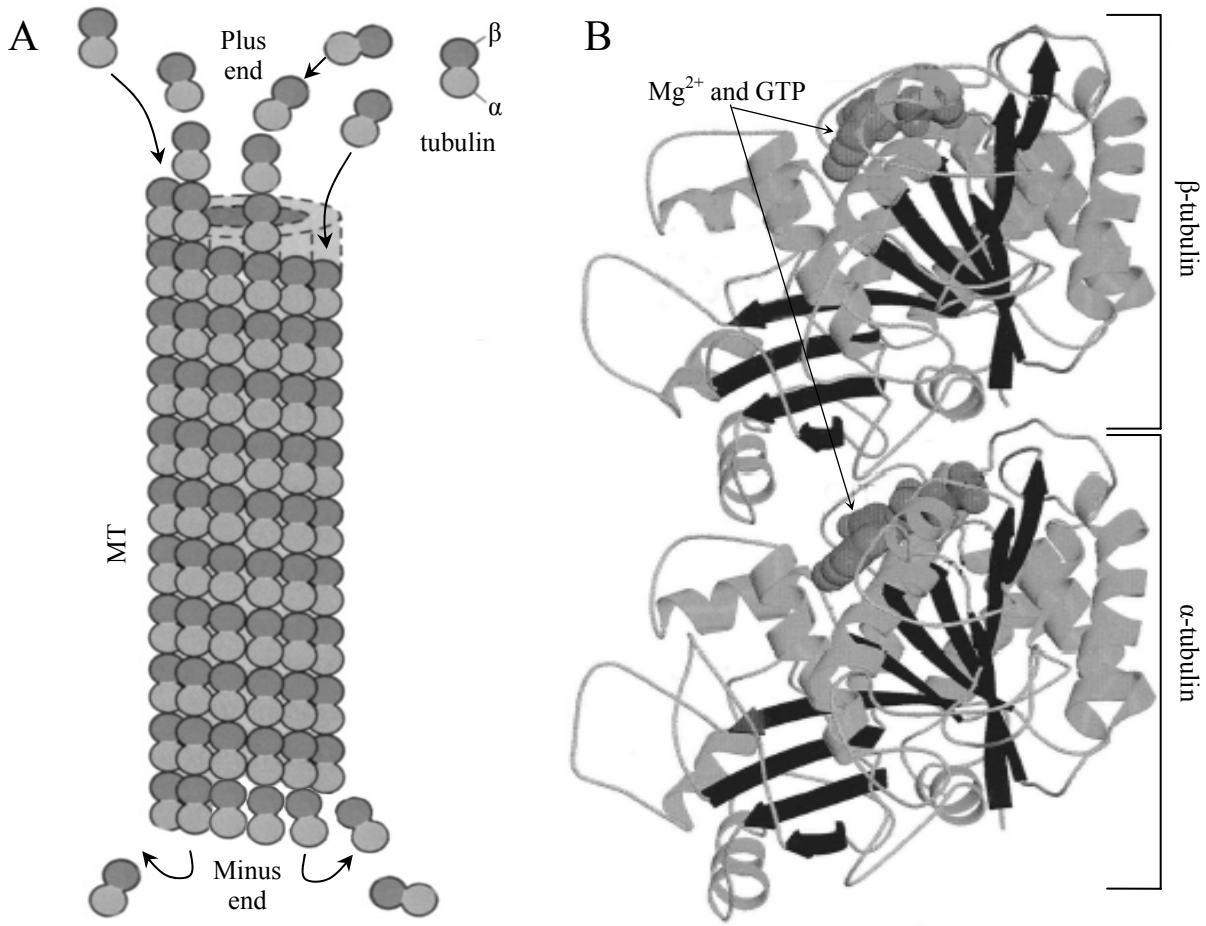

Figure 1. (A) MT structure and dynamic. Tubulins can incorporate into the MT or leave it on both ends (after Alberts et al., 1994). (B) Ribbon diagram of a tubulin heterodimer. The β-sheets appear as dark arrows, the α-helices as turning stripes (after Nogales et al., 1999).

The *Kavar*^{D} mutations revealed novel function of the α-tubulin^{4} isotype in the Drosophila embryo. In the wild type embryo the sperm introduced basal body becomes to function as the centrosome and organizes the formation of several hundred μm long so-called prominent

sperm aster MTs that serve as a route for shipment of the female pronucleus to close vicinity of the male pronucleus (Foe *et al.* 1993). Following centrosome replication the daughter centrosomes migrate along the nuclear perimeter to opposite poles and organize the spindle apparatus in which several of the MTs are well over 10 μm long (Foe *et al.* 1993; Figure 2). Although eggs of the *Kavar*^{18c}/+ females appear normal and are fertilized as in wild type, embryogenesis comes to a standstill soon after commencement and a monopolar spindle appears in each of the "die at start" embryos with two nearby located centrosomes embedded in a tassel of 3-5 μm short straight MTs. Since *Kavar*^{18c} has been shown to be of dominant negative nature (i.e. the *Kavar*^{18c}-encoded E82K-α-tubulin^4 molecules participate in the same process and hinder function of the normal α-tubulin^4 molecules) it may be suggested that α-tubulin^4 is required for the formation of lengthy MTs. Indeed, a tassel of short MTs with two closely located centrosomes forms in every egg of the *kavar*^{null}/– females which do not carry functional *αTub67C* gene (– stands for a deficiency that removes *αTub67C* and a few adjacent genes).

The lack of lengthy MTs in eggs of the *kavar*^{null}/– females is surprising knowing that α-tubulin^4 comprise only about 20% of the α-tubulin pool in the Drosophila eggs (Matthews *et al.* 1989). Although there is plenty of α-tubulin^1 and α-tubulin^3 in every Drosophila egg - encoded by the constitutively expressed and evolutionary highly conserved α-tubulin genes *α-tubulin84B* and *α-tubulin84D* - yet those do not support the formation of lengthy MTs. What makes α-tubulin^4 special? What is its function at the beginning of embryogenesis? Where is it localized in the early embryo? How do E84K-α-tubulin^4 molecules block the formation of lengthy MTs? Is function of α-tubulin^4 restricted to early embryogenesis? To answer the former questions we made use of two mutant *α-tubulin67C* alleles (*Kavar*^{18c} and the recently described *kavar*^{null}) as tools to understand the role of α-tubulin^4 in the formation and function of lengthy MTs. As reported in the present thesis, α-tubulin^4 is accumulated in the lengthy MTs that embrace the nuclear envelope, and suggest that they are in generation of the forces that push apart the daughter centrosomes to opposite poles along the nuclear perimeter comes from the fast growing interpolar MTs in the early cleavage embryos. It appears - based on results of in vitro tubulin polymerization assays - that α-tubulin^4 is actually required for rapid formation of lengthy MTs. Since the time available for tubulin polymerization is very short during the initial cleavage divisions (Edgar and Datar 1996; Ji et al., 2004; Tadros and Lipshitz 2005) and tubulin polymerization proceeds slowly in absence of α-tubulin^4 only short MTs can form. We also report that the need for α-tubulin^4 is limited to the initial cleavage divisions. Once the cleavage nuclei populate the egg cortex forces other than the growing

interpolar MTs accomplish separation of the daughter centrosomes (Cytrynbaum et al., 2003). The ectopically expressed *Kavar*^{18c}-encoded E82K-α-tubulin^{4} molecules become incorporated into the MTs nevertheless they do not disrupt MT associated functions in imaginal disc and neuroblast cells.

MATERIALS AND METHODS

The *Kavar*^{D} and the *kavar*^{r} alleles

The *Kavar*^{D} alleles were isolated in a screen for EMS-induced dominant female-sterile mutations (Table 1). The *kavar*^{r} revertant alleles were induced following second mutagenesis - by EMS or by X-rays - of the *Kavar*^{D} mutations assuming that the *Kavar*^{D} alleles are of gain-of-function nature and that the *kavar*^{r}/+ heterozygous females are viable and fertile (Table 1; Erdélyi and Szabad 1989). The *Kavar*^{18}/+, *Kavar*^{18}/– and the *kavar*^{null}/– females were produced in standard genetic crosses. For explanation of the genetic symbols see Lindsley and Zimm (1992) and the FlyBase at http://flybase.bio.indiana.edu. The Drosophila cultures were raised on standard food and kept on 25°C.

Table 1. The *Kavar*^{D} and the *kavar*^{r} alleles

Kavar^{D} allele	Founder chromosome	Revertant *kavar*^{r} alleles	
		EMS-induced	X-ray induced
Kavar^{18c}	Wild type (Canton-S)	*kavar*^{re11}, *kavar*^{re12}	-
Kavar^{21g}	*mwh e* labeled	~~*kavar*^{re21}~~, *kavar*^{re22}	*kavar*^{rX21}
Kavar^{21l}	*mwh e* labeled	*kavar*^{re31}	-

Notes:

- *kavar*^{re21} proved to represent a recombinant chromosome carrying the normal *Kavar* gene and was omitted from the present study.

- *kavar*^{rX21} was induced as described in Erdélyi and Szabad 1989. It is a complete loss-of-function allele and is referred here as *kavar*^{null}.

Mapping with duplications and deficiencies

To determine position of the *Kavar*^{D} mutations we generated *Kavar*^{D}/+/*Dp*$^{+}$ females that carried - in tandem duplications - different segments of the left arm of the 3rd chromosome and studied their embryo and offspring production. Once *Dp(3;3)S2a2* located *Kavar*^{D} to the 66D-67E cytological region we carried out deficiency mapping in which *kavar*^{r}/*Df(3L)* (= *kavar*^{r}/–) hemizygous females were generated and their offspring production was analyzed (see Figure 4). Except *Df(3L)55* and *Df(3L)21m*^{rX1}, the deficiencies are described in Lindsley and Zimm (1992) and in the FlyBase. *Df(3L)55*, that removes the 67B11-13 cytological region, originated through imprecise excision of the P*lacw*890/4 element (Kuhfittig, unpublished). P*lacw*890/4 resides in the 67B11 cytological region (Deák *et al.* 1997). *Df(3L)21m*^{rX1} is an X-ray induced revertant allele of *Damasa*^{21m}, a dominant female sterile mutation; It removes the 67B13-67C4 cytological region (Máthé, E. unpublished).

The *Kavar*$^{+}$ transgenes

To generate transgenes (TG) that include - one by one - the four genes in the 67B11-13 cytological region we isolated genomic fragments from a λ library. PCR products representing different sequences in the 67B11-13 region were used as probes to identify the appropriate λ clones. The PCR primers were synthesized on the basis of the Drosophila genome sequence (Adams *et al.* 2000). Fragments including one of the four genes with the regulatory sequences were isolated, cloned into the *CaSpeR* vector with the *mini-white* marker gene and germ line transformants were generated by standard procedures. (Features of the transgenes are summarized in Table 2.) To determine whether or not the transgene included the *Kavar*^{D}-identified gene we generated *Kavar*^{D}/+; *TG* as well as *kavar*^{r}/–; *TG* females which carried a transgene with one of the four genes in the 67B11-13 region. We assumed that if the transgene carried the *Kavar*^{D}-identified gene, fate of the embryos of the *Kavar*^{D}/+; *TG* and the *Kavar*^{D}/+/*Dp(3;3)*S2a2 females will be very similar and that the *kavar*^{r}/–; *TG* females will be fertile.

Table 2. Features of the transgenes covering the 67B11-13 region

Gene included in the transgene	G_0 parents tested	Transgene lines	Chromosomal location			
			X	2nd	3rd	4th
CG16717	79	1	0	0	1	0
α-tubulin67C	113	5	0	3	2	0
CG6767	104	8	3	5	0	0
UbcD4	157	10	1	1	7	1

Cytoplasm injections

To visualize effects of the mutant cytoplasm, we injected about 300 pl cytoplasm (~ 3% total egg volume) from eggs of *Kavar*^{18c}/– hemizygous females into the posterior region of wild type embryos (as described in Tirian *et al.* 2000) in which the MTs were highlighted by tubulin-GFP (Grieder *et al.* 2000). The donor embryos were less than 30 min old and the injected embryos were either in the 7th-9th cleavage cycle of embryogenesis with nuclei still deep down in the egg cytoplasm or in the 11th-13th cycle in the egg cortex (Foe *et al.* 1993). As control cytoplasm of wild type embryos was injected. Effect of the injected cytoplasm was followed in time through series of optical sections generated in a ZEISS LSM410 confocal microscope. The injections were done on 20°C.

Diameter of the embryonic nuclei

To determine the diameter of the cleavage nuclei we collected embryos from two strains: (i) *w*^{1118} and (ii) histone-GFP in which a transgene encodes synthesis of a fusion protein between histone H2Av and GFP (Clarkson and Saint, 1999). Nuclear diameter of the *w*^{1118} embryos were measured throughout the cleavage cycles following fixation with methanol and staining with DAPI, and also for the 10th-13th cycles in live histone-GFP embryos. For cycles 1-5 all nuclei of at least twenty embryos were measured and for the later stages at least ten nuclei of the minimum of ten embryos. Nuclear diameter of the fixed and the live embryos were basically identical and were pooled in Figure 15.

Immunological techniques

For immunological detection of tubulins we followed standard techniques (Sambrook *et al.*, 1989). Briefly, protein samples were prepared from 0-2 hour old embryos. The eggs were dechorionated by chlorox, homogenized in SDS buffer and boiled for 10 min before SDS denaturing gel electrophoresis. To detect α-tubulins - both in Western blots and in confocal microscopy - we used the DM1A monoclonal mouse anti-α-tubulin (SIGMA) antibody. The secondary anti-mouse antibodies were labeled either with alkaline phosphatase (Roche), FITC or AlexaFlour633 (SIGMA). To specifically detect α-tubulin^4, we synthesized an olygopeptide based polyclonal anti-α-tubulin^4 in rabbits. The olygopeptide represented the last 14 C-terminal amino acids specific for α-tubulin^4: DNAEEGGDEDFDEF. The antibody was affinity-purified on a protein-A column and on nitrocellulose strips followed by low pH elution according to Smith and Fisher (1984). For confocal microscopy non-specific activities

from the protein-A purified antibody samples were depleted by preincubation of the antibody before use with fixed and permeabilized eggs that derived from *kavar*^{null}/– females that lacked α-tubulin^{4}. Anti-α-tubulin^{4} antibody allows clear distinction - both in Western blots and in confocal microscopy - between α-tubulin^{4} and α-tubulin^{1} and α-tubulin^{3}, the α-tubulin isotypes present in the embryos. Since the C-terminal part is identical in α-tubulin^{4} and E82K-α-tubulin^{4} the anti-α-tubulin^{4} antibody equally efficiently recognizes the two types of molecules. In the Western blot the labeled proteins were detected in a Typhoon 8600 device (Amersham).

To analyze structures in the eggs/embryos the chorion was removed either by a brief chlorox treatment or by a double-stick tape. After removal of the chorion the embryos were fixed in a mixture of 1:1 4% paraformaldehyde and heptane or in a 1:1 mixture of methanol and heptane. The vitelline membrane was removed subsequently by agitation in a mixture of heptane and methanol. Before processing for analysis the embryos were stored in methanol at -20°C. For microscopy the embryos were rehydrated and rinsed in PBST. To block nonspecific staining the embryos were incubated in 1% BSA (SIGMA) in PBST for 90 min at room temperature. For detection of the centrosomes and the MTs we incubated the embryos in the DM1A mouse monoclonal anti-α-tubulin (1:1000, overnight at 4°C) or in the anti-centrosomin (CNN) antibody (1:1000; Heuer *et al.* 1995) or in the anti-α-tubulin^{4} (1:200) primary antibody. The primary antibodies were applied in 1% BSA in PBST. After several rinses in PBST the embryos were incubated in secondary antibodies for 3 hours at room temperature or overnight on 4^{o}C. The following secondary antibodies were either anti-mouse or anti-rabbit IgG (SIGMA) and labeled either by FITC, Texas-red or AlexaFlour633. To detect DNA we stained the embryos with DAPI following incubation in the secondary antibody. Following several rinses in PBST the embryos were mounted in Aqua PolyMount (Polysciences Inc). Optical sections were generated in a ZEISS LSM410 and in an Olympus FV1000 confocal microscope.

Ectopic expression of E82K-α-tubulin^{4}

To see whether ectopic expression of the *Kavar*^{18c}-encoded E82K-α-tubulin^{4} molecules have the same effect on cells as on early cleavage embryos, we generated both *UAS-Kavar*^{18c} and, as control, *UAS-α-tubulin67C* transgenes and expressed those with tissue specific *Gal4* drivers (Duffy, 2002; FlyBase). For generation of the UAS-*Kavar*^{18c} and the *UAS-α-tubulin67C* transgenes we combined a multiple UAS containing DNA fragment with a cDNA that contained either the *Kavar*^{18c} mutation or the normal *α-tubulin67C* coding sequences,

cloned into the *CaSpeR* vector with the *mini-white* marker gene and generated germ line transformants by standard procedures. Features of the *UAS-α-tubulin67C* and the *UAS-Kavar^{18c}* transgenes are summarized in Table 3.

Table 3. Features of the *UAS-α-tubulin67C* and the *UAS-Kavar^{18}* transgenes

Transgene	Transgenic line			Driven by *α-tub84B-Gal4*[1]
	Total	Chromosome location	Homozygous	
UAS-α-tubulin67C	9	1x1st; 4x2nd; 4x3rd	Viable, fertile	Renders *kavar^{null}*/– females fertile[2]
UAS-Kavar^{18c}	10	2x2nd; 8x3rd	Viable, fertile	Renders females sterile

[1] Lee and Lou 1999.
[2] Only for transgenes linked to the 1st (= X) and to the 2nd chromosome.

For ectopic expression of E82K-α-tubulin^4 (or α-tubulin^4 as control) we generated zygotes, through genetic crosses, in which different *Gal4* drivers assured tissue specific expression of a *UAS-Kavar^{18}* (or a *UAS-α-tubulin67C*) transgene and determined whether the *Gal4*; *UAS-Kavar^{18}* flies are viable, possess developmental abnormalities or female-sterility. To determine whether E82K-α-tubulin^4 (or α-tubulin^4) become incorporated into the spindle apparatus in the neuroblasts we generated larvae in which the *elav-Gal4* driver (Lou *et al.*, 1994) drove a *UAS-Kavar^{18}* (or a *UAS-α-tubulin67C*) transgene. The ventral ganglion was dissected from late third instar larvae, fixed in 4% paraformaldehyde, incubated in both anti-α-tubulin^4 - to label E82K-α-tubulin^4 (or α-tubulin^4) - and in the DM1A antibody to label α-tubulin^1 and α-tubulin^3 for microscopic analysis and determined whether E82K-α-tubulin^4 (or α-tubulin^4) became incorporated into the MTs of the spindle apparatus.

In vitro MT polymerization assay

In the *in vitro* tubulin polymerization experiments we collected eggs from three types of females. The +/– control females carried one copy of the normal *αTub67C* gene, the *kavar^{null}*/– females did not carry functional *αTub67C* gene and the *Kavar^{18c}*/– females carried only the E82K-α-tubulin^4-encoding dominant female sterile mutant allele. To achieve maximum similarity in egg cytoplasm status and high egg production rate the females were

collected as virgins and were kept together with sterile X0 males (Liu and Kubli, 2003). For isolation of tubulins we collected eggs for one hour and than processed according to Cullen et al. (1999). Briefly, after removal of the chorion with bleach the eggs/embryos were homogenized in BRB80 buffer (80 mM Pipes, 2 mM $MgCl_2$ and 1 mM EGTA) containing a cocktail of protease inhibitors (PI) and 1 mM dithiothreitol (DTT). The homogenate was incubated on 4^{o}C for 30 min and spun at 140,000g at 4-8^{o}C for 30 min to remove debris and heavy particles. The supernatant was kept as egg extract.

We conducted two types of in vitro polymerization assays. (1) In the first assay we used taxol, a MT stabilizing agent, to have all the tubulins incorporated into the MTs. One mM GTP and a final concentration of 20 μM taxol were added to the egg extract before incubation on room temperature to induce polymerization of the tubulins and to stabilize the forming MTs. The MTs and associated proteins were pelleted by spinning at 80,000g for 30 min through a 30% sucrose cushion in the BRB80 buffer. The egg extract, the pellet (i.e. the MTs) and the supernatant were analyzed by SDS PAGE and Western-blot using anti-α-tubulin primary and fluorescently labeled secondary antibodies. (2) To test the effect of E82K-α-tubulin^4 and normal α-tubulin^4 on polymerization we analyzed MT formation in extracts of unfertilized eggs. Briefly, PI cocktail, DTT and EGTA to a 1 μM final concentration were added to 50-100 μl 0-1h old eggs before homogenization. The homogenized samples were stored on 4°C for 30 minutes to have the MTs disassembled. The homogenates were centrifuged next three times (22,000g on 4°C for 10 minutes) until clearing. Tubulin concentration of the egg extracts was about 1μM according to a semi-quantitative analysis of Coomassie Blue stained SDS PAGE gels. The samples were stored on -70°C until use. To produce labeled MTs we mixed 5 μl of an extract with 0.5 μl of 10x EMM mix [final concentrations: 5% DMSO, + 0.5 mM GTP, + 4 mM $MgCl_2$, 1 mM EGTA, 0.3 μM Oregon-green 514 (Molecular Probes) or 0.3 μM rhodamine labeled (Cytoskeleton) bovine tubulin]. To test the effect of E82K-α-tubulin^4 on MT formation we transferred the preparations (from eggs of +/–, *Kavar*^{18c}/– and *kavar*^{null}/–) to 37°C and incubated for 30 minutes in the presence and in the absence of taxol. In "the presence of taxol" actually meant 0.2 μM taxol at the beginning, to stabilize the forming MTs. After 15 minute incubation the taxol concentration was raised to 2 μM according to the Mitchison laboratory protocols (http://mitchison.med.harvard.edu). To test the effect of α-tubulin^4 on polymerization kinetics we incubated two types of egg extracts (from eggs of +/– and *kavar*^{null}/– females) for 2, 5, 7.5, 10, 12.5, 15, 20 and 30 minutes on 32^{o}C. The polymerization reactions were terminated by diluting the reaction 20 fold with 80T (BRB80+10 μM taxol). Three μl samples were

immediately mixed with 3 µl Aqua Polymount on a slide, covered with a coverslip and images were collected with an Olympus IX71 fluorescent microscope. Lengths of MTs were measured by the ImageJ image analyzer program. The data were analyzed by the SPSS™ statistical program.

RESULTS

The *Kavar^{D}* mutant phenotypes

Although eggs of the *Kavar^{18c}*/+ females are fertilized as in wild type (as was detected by a sperm-tail specific antibody; data not shown) embryogenesis does not commence inside the eggs. The sperm-introduced centrosome divides and daughter centrosomes form (Figure 2). Unlike in wild type, where the centrosomes move apart over the perimeter of the nuclear envelope (Foe *et al.* 1993), the daughter centrosomes are closely located in every egg of the *Kavar^{18c}*/+ females and are closely associated with a tassel of MTs with over-condensed chromosomes inside. The above-mentioned structure is characteristic of the collapsed spindles (Sharp *et al.* 1999).

Less severe defects develop in eggs of the *Kavar^{21g}*/+ and *Kavar^{21l}*/+ females as seen in case of *Kavar^{18c}*. Embryogenesis does not commence in about 20% of the eggs. In about 30% of the eggs development comes to an end following 1-8 cleavage divisions inside the egg cytoplasm prior to migration of the cleavage nuclei into the cortex. In about 50% of the eggs 1-3 islands of cleavage nuclei manage to migrate into the egg cortex where they, as in wild type, accomplish the four additional cleavage divisions populating variable sized territories of the egg cortex (Figure 3).

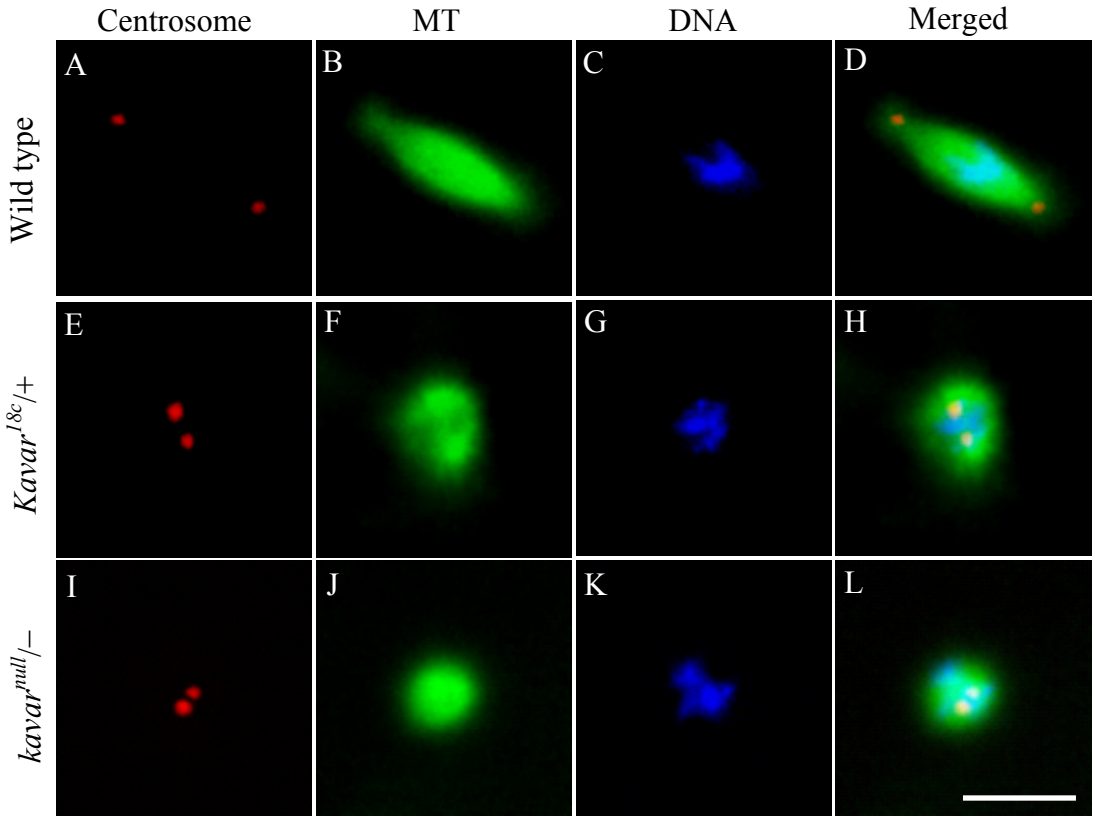

Figure 2. Components of the first cleavage spindle in a wild type (A-D), in a *Kavar*^{18c}/+ (E-H) and in a *kavar*^{null}/− derived embryo (I-L). Centrosomes, MTs and the DNA are shown in stacked optical sections. Note that basically identical defects emerge in eggs of the *Kavar*^{18c}/+ and the *kavar*^{null}/− females. (Scale bar = 10 μm.)

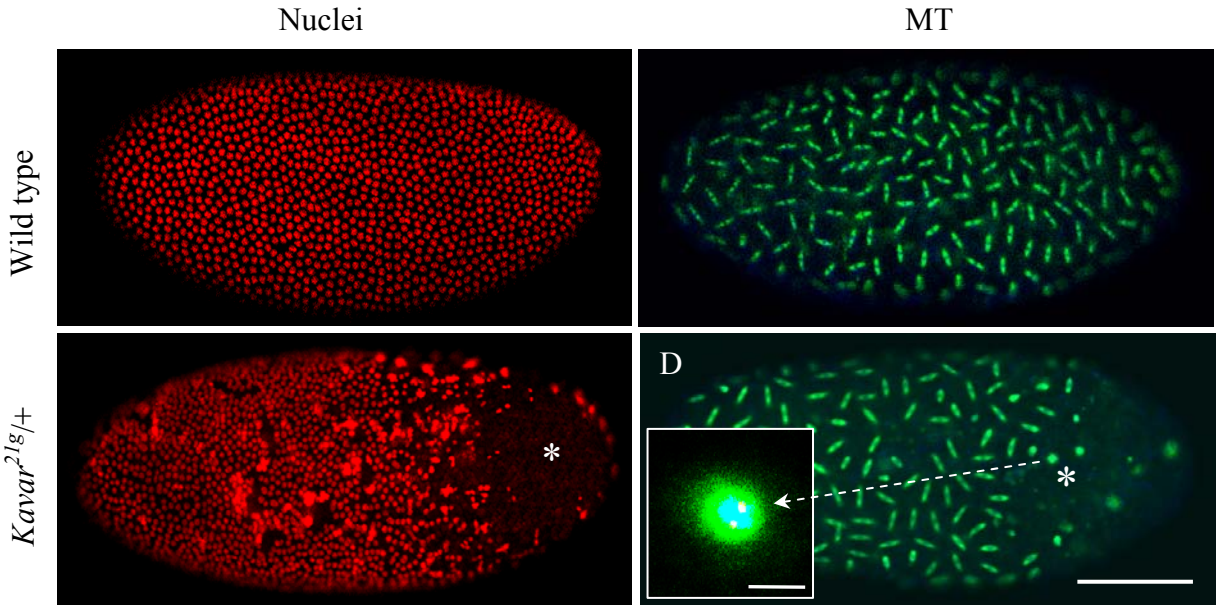

Figure 3. Distribution of nuclei and MTs in embryos of wild type (A, C) and *Kavar*^{21g}/+ females (B, D). Several of the cleavage nuclei fail to migrate to the egg cortex in the *Kavar*^{21g}/+ derived embryos thus areas without nuclei and mitotic spindles (*) appear. DNA of the "left behind" nuclei decomposes eventually and appears as large red spots (B). The insert in D shows a merged close up picture of a collapsed spindle with the tubulin (green), DNA (blue) and centrosomes (red). (Scale bar = 50 μm for A-D and 10 μm in the insert in D.)

While cellularization proceeds normally over the nucleated areas and variable sized blastoderm-like sheets of cells form, large territories of the egg cortex remain devoid of nuclei and cells. Apparently at least some of the cells behave normally since 6-9% of the embryos turn light brown indicating differentiation beyond the blastoderm stage (Wieschaus and Nüsslein-Volhard 1986; Table 4). Indeed, all the larval landmark structures differentiate, although in different embryos. Among embryos which derived from a cross between *y*/*y*; *Kavar*^{21g}/*y*$^{+}$*TM3, Sb Ser* females and *y*/Y; +/+ males and developed some head skeleton and/or ventral setae, allowing distinction between *y* and *y*$^{+}$, roughly 50% were yellow (*Kavar*^{21g}/+) and 50% yellow^{+} (+/*y*$^{+}$*TM3, Sb Ser*) showing that *Kavar*^{21g} is a typical maternal-effect lethal mutation. Under those areas where nuclei failed to migrate to the egg cortex the cleavage spindles collapse, centrosomes detach from the spindle pole, tri-, multipolar and fused spindles form. Obviously, even the most advanced embryos die and hence the *Kavar*^{D}/+ females are invariably sterile.

The loss-of-function mutant phenotype

The finding that the *kavar*^{r}/– females are sterile clearly shows that the normal *kavar* gene product is maternally provided and is required during embryogenesis. Sterility of the *kavar*^{r}/– females opened the possibility to determine the complete loss of function phenotype. While in some eggs of the *kavar*^{r}/– females some very abnormal embryonic development was apparent, embryogenesis did not commence in eggs of the *kavar*^{null}/– females. (The molecular nature of *kavar*^{null} is described below.) The mutant phenotype seen in eggs of the *kavar*^{null}/– females was basically identical to that described for the *Kavar*^{18c}/+ females (Figure 2) and shows that the *Kavar*^{18c} encoded mutant gene product eliminate function of the normal counterpart.

Mapping of the *Kavar*^{D} and the *kavar*^{r} alleles

The *Kavar*^{D} mutations were mapped to the left arm of the 3rd chromosome (3L; Erdélyi and Szabad 1989). For more precise localization of *Kavar*^{D} we constructed *Kavar*^{21g}/+/*Dp* females in which the duplications (*Dp*) included different segments of 3L. It was our hope that some of the duplications will include a normal *kavar*$^{+}$ gene copy, which will reduce severity of the *Kavar*^{D}-associated defects. With the exception of *Dp(3;3)S2a2* 6-9% the eggs turned brown as in eggs of the *Kavar*^{21g}/+/*Dp* females. However, in case of the *Kavar*^{21g}/+/*Dp(3;3)S2a2* females, 62% of the eggs turned brown (Table 1) showing that *Kavar*^{21g} belongs to the dominant negative (antimorph) class of the gain-of-function mutations. (Among eggs of the

Kavar^{18c}/+/*Dp(3;3)S2a2* females one in about a thousand eggs turned slightly brown.) The dominant negative nature of the *Kavar*^{D} mutations implies that the normal and the *Kavar*^{D}-encoded mutant gene products participate in the same process such that the mutant gene product hinders function of the normal one. The dominant negative nature of *Kavar*^{D} is also shown by two further observations: (1) embryogenesis is terminated before the 5th cleavage division in eggs of the *Kavar*^{21g}/– hemizygous females and (2) when injected into wild type embryos cytoplasm of the *Kavar*^{18c}/– derived eggs poisons the embryos through production of collapsed spindles (see below).

Table 4 Effects of duplications and transgenes on *Kavar*^{21g}-imposed female sterility

Genotype		Offspring production			Egg production			
						Eggs		
		Females tested	Test period (days)	Offspring	Single females tested	Total	Dark	Average dark (%) ± SD
Kavar^{21g}/+		987	19231	0	10	1127	55	7.8 ± 6.1
Kavar^{21g}/+/*Dp(3;3)S2a3*		26	398	0	19	2014	183	9.1 ± 6.5
Kavar^{21g}/+/*Dp(3;3)S2a2*		25	285	0	13	1205	754	62.3 ± 6.0*
Kavar^{21g}/+ plus a transgene	CG16717	207	3931	0	23	3611	235	6.5 ± 4.4
	α-tubulin67C	216	3402	0	17	2909	1286	40.6 ± 3.2*
	CG6767	663	10997	0	34	2867	315	9.4 ± 4.9
	UbcD4	279	5270	0	11	858	54	6.3 ± 4.1

* = significantly different from the background frequency (t probe, $P < 0.01$)

Comparison of brown embryo production of the *Kavar*^{21g}/+ females, which carried either of the duplications *UV7*, *S2a2* or *S2a3,* clearly showed that *Kavar*^{21g} resides in the 67B-C cytological region (Figure 4). For more precise localization of the *Kavar*^{D}-identified gene we combined the *kavar*^{r} revertant alleles with deficiencies (–) that removed different segments of the 67B-C region (Figure 4). The *kavar*^{r}/– females in which the 67B11-67C4 region was removed by the deficiency *Df(3R)55*, were invariably sterile locating the *Kavar* gene into that segment of 3L.

Df(3R)55 removes a ca. 30kb segment of the genome. The Drosophila genome project predicts four genes in the region (Adams *et al.* 2000; Figure 4). We generated transgenes (TG), which included genomic segments with one of the four genes (Table 2). The *Kavar*^{21g}/+; TG females that carried the *αTub67C* gene in the transgene, produced - like the

Kavar^{21g}/+/*Dp(3;3)S2a2* females - high frequencies of brown embryos showing that the *Kavar*^{D} mutations identify the *αTub67C* gene (*α-Tubulin* at 67C; see the FlyBase at http://flybase.bio.indiana.edu) of *Drosophila melanogaster* (Table 3; Venkei and Szabad, 2005). The conclusion is confirmed by the following results. (1) The *kavar*^{r}/− females with a single copy *αTub67C* transgene are fully fertile. (2) The *kavar*^{r} alleles do not complement the formerly described loss-of-function *αtub67C*$^{-}$ and *tomaj*^{r} alleles (Matthews *et al.* 1993; Máthé *et al.* 1998). (3) Sterility of the *αtub67C*$^{-}$/− and the *tomaj*^{r}/− hemizygous females is fully rescued by a single *αTub67C* transgene.

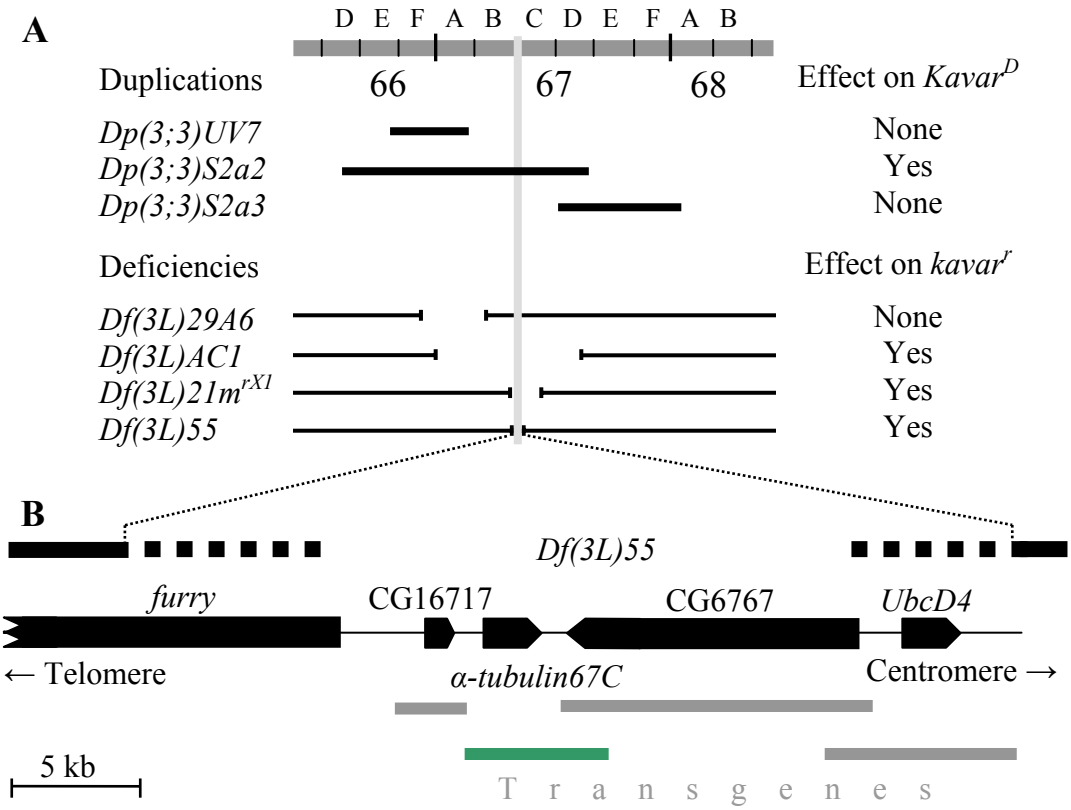

Figure 4. Mapping the *Kavar*^{D} alleles with duplications (thick, solid bars) and the *kavar*^{r} alleles with deficiencies (thin broken bars) on the cytological map (A). Gaps in the deficiencies illustrate the missing segment of the chromosomes. Genes uncovered by the *Df(3L)55* deficiency and transgenes that include one of the four genes (B). (The dashed parts in the *Df(3L)55* deficiency show sequences that may or may not be removed from the DNA.)

Molecular nature of the *Kavar*^{D} and *kavar*^{null} alleles

To elucidate the molecular nature of *Kavar*^{18c}, *Kavar*^{21g}, *Kavar*^{21l} and *kavar*^{rX21}, we isolated DNA from *Kavar*^{18c}/–, *Kavar*^{21g}/–, *Kavar*^{21l}/– and *kavar*^{rX21}/– hemizygous males as well as

from the founder chromosomes (Table 1), PCR amplified and sequenced the *αTub67C* gene. It turned out that *Kavar*^{18c} originated through a single base pair substitution G^{244}→A mutation and the concomitant replacement of Glu^{82} by Lys (E82K) in the otherwise normal sized protein composed from 452 amino acids. *Kavar*^{21g} and *Kavar*^{21l} originated through a G^{1276}→A transition and replacement of Glu^{426} by Lys (E426K). Since *Kavar*^{21g} and *Kavar*^{21l} were generated and isolated in the same mutagenesis experiment (Erdélyi and Szabad 1989) they represent a small cluster of the same mutation. The first known null mutant allele in the *αTub67C* gene - *kavar*^{rX21}- originated through the deletion of four base pairs (C^{56}TGC) near the 5' end of the coding sequence. The deletion leads to a frame shift from the 19th code and the formation of a non-functional peptide composed from 34 amino acids. Apparently *kavar*^{rX21} is a complete lack-of-function (amorph) allele, the only such allele in the *αTub67C* gene, and is labeled here as *kavar*^{null}.

Cytoplasm injections

To reveal the role of α-tubulin^4 we injected small cytoplasm samples from eggs of wild type (as control) and *Kavar*^{18c}/– hemizygous females into live embryos in which the microtubules were highlighted by GFP-tagged α-tubulin^1. Two types of cytoplasm injections were done. (1) In the first set of injections detailed effect of the injected cytoplasm was not followed in time. The injected embryos were engaged in the 7th-9th cleavage cycle. Toxicity of the *Kavar*^{18c}/– derived egg cytoplasm was apparent since while larvae hatched from almost every of the 185 embryos injected with wild type egg cytoplasm not a single larva hatched from the 138 embryos injected with E82K-α-tubulin^4 containing cytoplasm. (2) In the second set of experiments we injected the cytoplasm samples into embryos in the 10th-11th cleavage cycle, with nuclei already in the egg cortex and analyzed effects of the injected cytoplasm in time lapse series of optical sections. In this experiment 20 embryos were injected with wild type, and 30 with *Kavar*^{18c}/– derived egg cytoplasm. The *Kavar*^{18c}/– egg cytoplasm had no effect on the already established mitotic spindles and did not disturb events of meta-, ana- or telophase (Figure 5). The observation excludes the possibility that the monopolar spindles originate through spindle collapse.

Injection of E82K-α-tubulin^4 containing cytoplasm invariably slowed down separation of the daughter centrosomes (Figure 5). Depending on - most likely - the local concentration of E82K-α-tubulin^4 changes in the microtubule formation pattern was abnormal: in about 50% of the injected embryos the partially separated centrosomes nucleated microtubules that remained short and straight and spindles never formed over the affected nuclei (Figure 5,

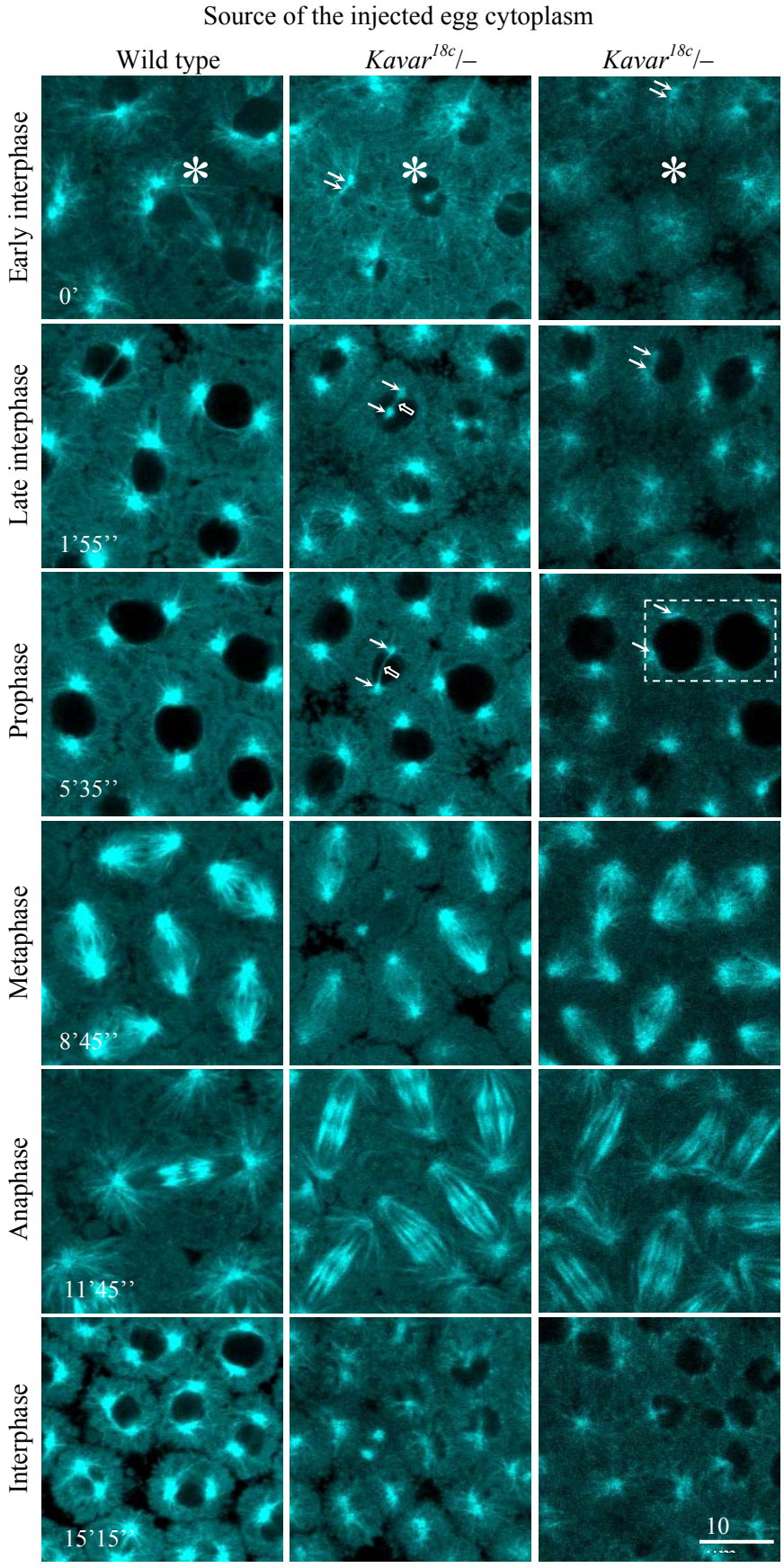

Figure 5. Time lapse series of optical sections throughout the 12th cleavage cycle following egg cytoplasm injection. The MTs were highlighted by α-tubulin[1]-GFP. The embryos were injected in anaphase of the 11th cleavage cycle. The injected egg cytoplasm samples were taken from a wild type (first column) or from a *Kavar*^{18c}/– derived egg (second and third columns). The E82K-α-tubulin[4] molecules (present in the *Kavar*^{18c}/– derived egg cytoplasm) slowed down separation of the daughter centrosomes, as labeled by white arrows. The partially separated centrosomes may either organize the formation of short MTs that never assemble to a spindle apparatus (as shown on the second column), or fail to localize the nuclei properly (see the adjoining nuclei in the dashed box of the last column) and lead to the formation of tripolar spindles. * labels the site of cytoplasm injection. The time after injection is shown in the optical sections of the first column. Arrows point to the centrosomes, open arrows point to the interpolar MT bundles.

second column). The defect is very similar to that seen inside eggs of the *Kavar*^{18c}/+ females. In less severe cases the slowed down centrosome failed to space the nuclei properly and as a consequence tripolar spindles formed by recruiting a centrosome of the adjoining nucleus (Figure 5, third column).

Surprisingly, the injected *Kavar*^{18c}/– derived egg cytoplasm did not do any harm to the 15 embryos that had accomplished the 12th or were engaged in the 13th (last) cleavage division, a feature that will be discussed in a subsequent paragraph.

Localization of α-tubulin^4 in wild type cleavage embryos

To visualize α-tubulin^4 throughout the cleavage cycles, we generated a polyclonal anti-α-tubulin^4 antibody by making use of the unique 14 amino acid long C-terminal segment of α-tubulin^4. The antibody is specific for α-tubulin^4 and does not recognize α-tubulin^1 and α-tubulin^3, the evolutionary highly conserved and constitutively expressed isotpyes (Figure 6). DM1A, the monoclonal anti-α-tubulin antibody, recognizes α-tubulin^1 and α-tubulin^3 but not α-tubulin^4 and thus the two antibodies allow side-by-side detection of the different α-tubulins (Figure 6).

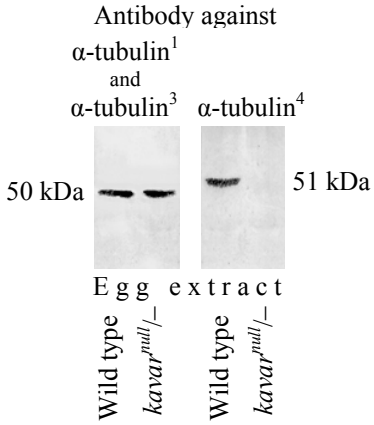

Figure 6. Specificity of the monoclonal DM1A and the anti-α-tubulin^4 polyclonal rabbit antibodies. As Western blot analysis revealed, DM1A recognizes the evolutionary highly conserved and constitutively expressed α-tubulin^1 and the α-tubulin^3 isotypes but not α-tubulin^4. Anti-α-tubulin^4 recognizes only α-tubulin^4. Note that there is no α-tubulin^4 in egg cytoplasm of the *kavar*^{null}/– females. (Dilutions were 500-fold for DM1A and 2000-fold for anti-α-tubulin^4.)

As summarized in Figure 7, all three α-tubulin isotypes are components of all types of MTs throughout the cleavage divisions. However, there is a significant enrichment of α-tubulin^4 in the so-called interpolar MTs which embrace the nuclear envelope during interphase and early prophase and push the daughter centrosomes along the nuclear perimeter to opposite poles (Figure 7 and 8; see also Scholey et al., 2003). Importantly, thickness of the interpolar MT bundle signal is uniform around the nuclear envelope (outside the centrosome regions) suggesting that several of the MTs run from centrosome to centrosome, between the two poles (Figure 8). Enrichment of α-tubulin^4 in the MTs embracing the nuclear envelope is a characteristic feature of the cleavage cycles.

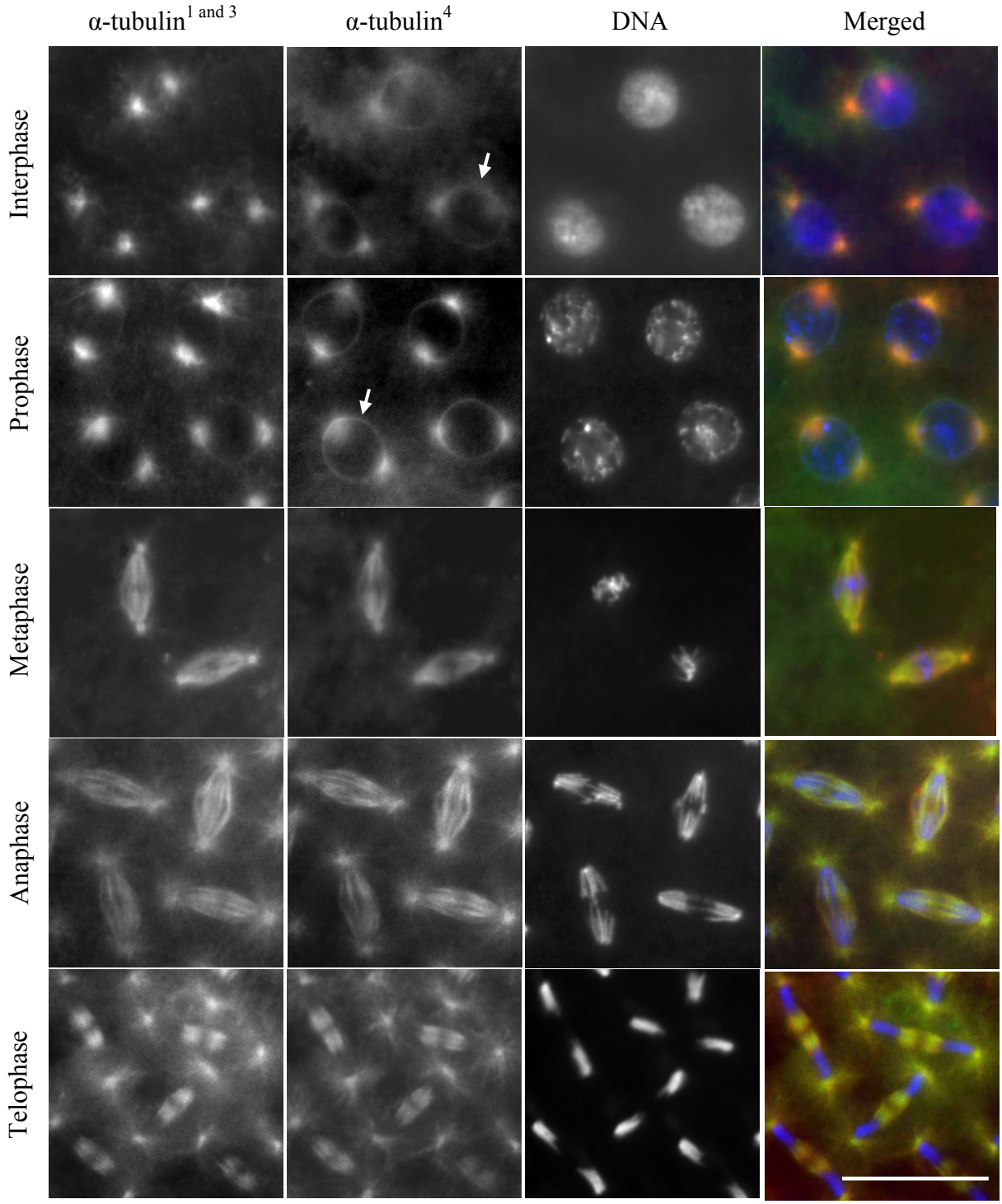

Figure 7. Distribution of α-tubulin[1], α-tubulin[3] and α-tubulin[4] throughout the 11[th] cleavage cycle in a Drosophila embryo. The constitutively expressed and evolutionarily highly conserved α-tubulin[3] and α-tubulin[4] isoforms were detected by the monoclonal antibody DM1A and α-tubulin[4] by a rabbit polyclonal antibody. In the merged panel red labels the constitutive α-tubulins, green shows α-tubulin[4] and the DNA appears in blue. Note accumulation (as indicated by arrowheads) of α-tubulin[4] in the long MTs that embrace the nuclear envelope in interphase and early prophase. (Scale bar = 20μm.)

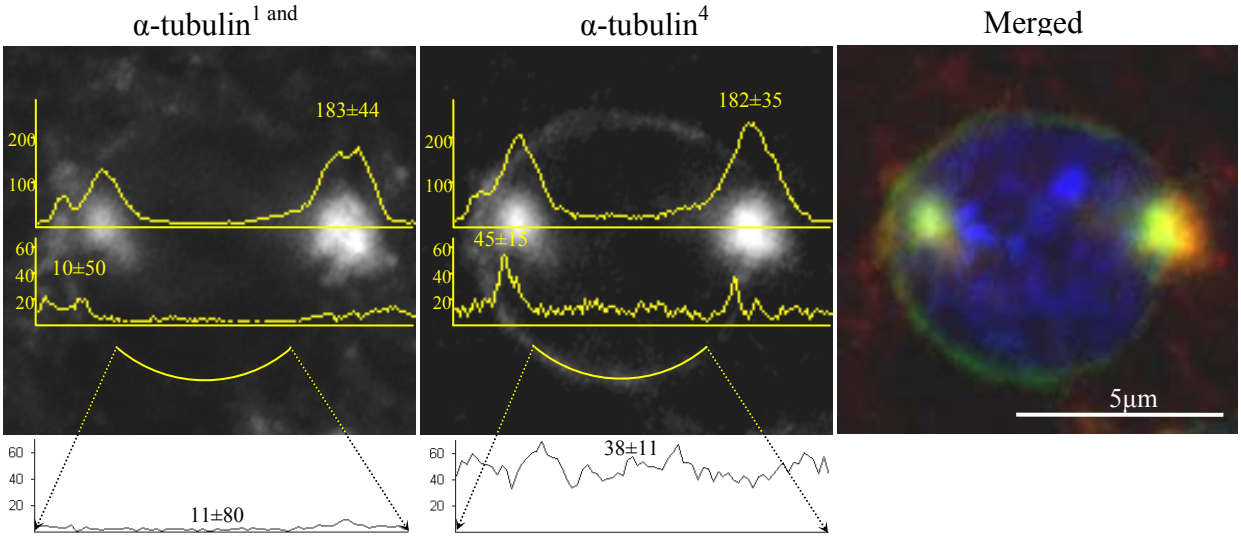

Figure 8. The maternal α-tubulin^4 isotype is enriched in the interpolar MTs. The α-tubulin^1 and α-tubulin^3 and also the α-tubulin^4 isotypes were made visible in fixed cleavage embryos as described in Figure 7 and analyzed in optical sections prepared in an Olympus FV1000 confocal microscope. (DNA was made visible by DAPI and appears blue in the merged picture.) To reveal the concentration of α-tubulin^1 and α-tubulin^3 as well as α-tubulin^4 over the nuclear region we set two lines: one across the centrosomes and another line crossing the interpolar MT region. An arc was also set to follow the region of the interpolar MTs. We than determined the distribution of signal intensities (that ranged between 0 and 255) in the pixels along the two lines and the arc. Pixel intensities reflect fluorescence intensities and the amount of the different types of tubulins. The curves over the lines illustrate intensity distributions for a single nuclear region. The intensity distributions along the arc appear over the straight lines below the pictures. Altogether 20 nuclear regions were analyzed: in five nuclei in each of four embryos. The peak intensities (average ± SD; n=40) over the centrosome regions and at the intersections in the interpolar MTs appear in the figure. Intensities along the arc were collected from 20 nuclei. The analysis revealed a highly significant accumulation of α-tubulin^4 in the interpolar MTs ($P<0.01$, t probe).

Incorporation of E82K-α-tubulin^4 into MTs that form in vitro and in vivo

To determine how E82K-α-tubulin^4 molecules exert their toxic action we carried out an *in vitro* MT polymerization assay. We prepared extracts from 0-30 min old embryos of +/– (as control, with one copy of the normal *αTub67C* gene) and *Kavar*^{18c}/– females and induced polymerization of MTs in the egg extracts by the addition of GTP and stabilized the forming MTs by taxol. The MTs were pelleted and the types of proteins in the pellets were separated through SDS PAGE gel electrophoresis. We than made use of Western blot analysis to detect α-tubulin^1 and α-tubulin^3 by the DM1A and α-tubulin^4 by its specific antibody. To distinguish the different α-tubulin isotypes we used secondary antibodies, one of which emitted green and

the other red fluorescent light. Results of the *in vitro* tubulin polymerization assay are summarized in Figure 9 and show that egg cytoplasm of the +/– and the *Kavar*^{18c}/– females contain about equal amounts of α-tubulins. Western-blot analysis did not detect α-tubulin in the supernatant showing that both the normal and E82K-α-tubulin^4, become incorporated into the forming MTs during *in vitro* polymerization. Apparently, and in agreement with the mutant phenotype, E82K-α-tubulin^4 does not exert its toxic effect throughout blocking MT formation. Rather, E82K-α-tubulin^4 becomes incorporated into the MTs and prevents formation of lengthy MTs.

As Figure 10 shows the α-tubulin^4 molecules are incorporated into the first embryonic spindle apparatus where they appear evenly distributed over the MTs. Notably E82K-α-tubulin4 also becomes incorporated into the MT tassels in eggs of the *Kavar*^{18c}/– females however they do not seem to support the formation of lengthy MTs (Figure 10).

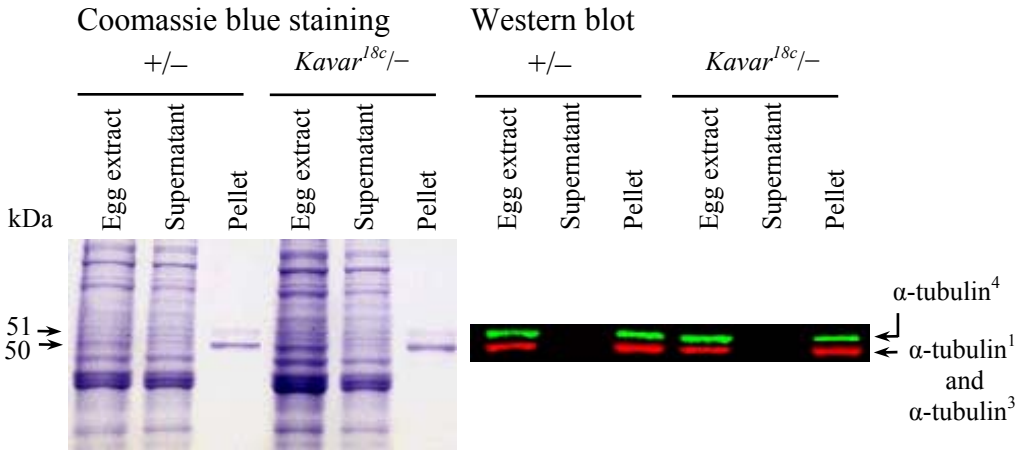

Figure 9. Results of the *in vitro* tubulin polymerization assay. MT formation was induced in extracts of +/– (with one normal *αTub67C* gene) and *Kavar*^{18c}/− females. The forming MTs were pelleted. Egg extracts, the supernatant and the MT-containing pellet were analyzed following SDS PAGE gel electrophoresis by Coomassie blue staining and by Western blot analysis. The α-tubulin^1 and the α-tubulin^3 isotypes were detected by the monoclonal DM1A primary and a red fluorescent secondary antibody, and α-tubulin^4 by a polyclonal primary anti-α-tubulin^4 and a green fluorescent secondary antibody.

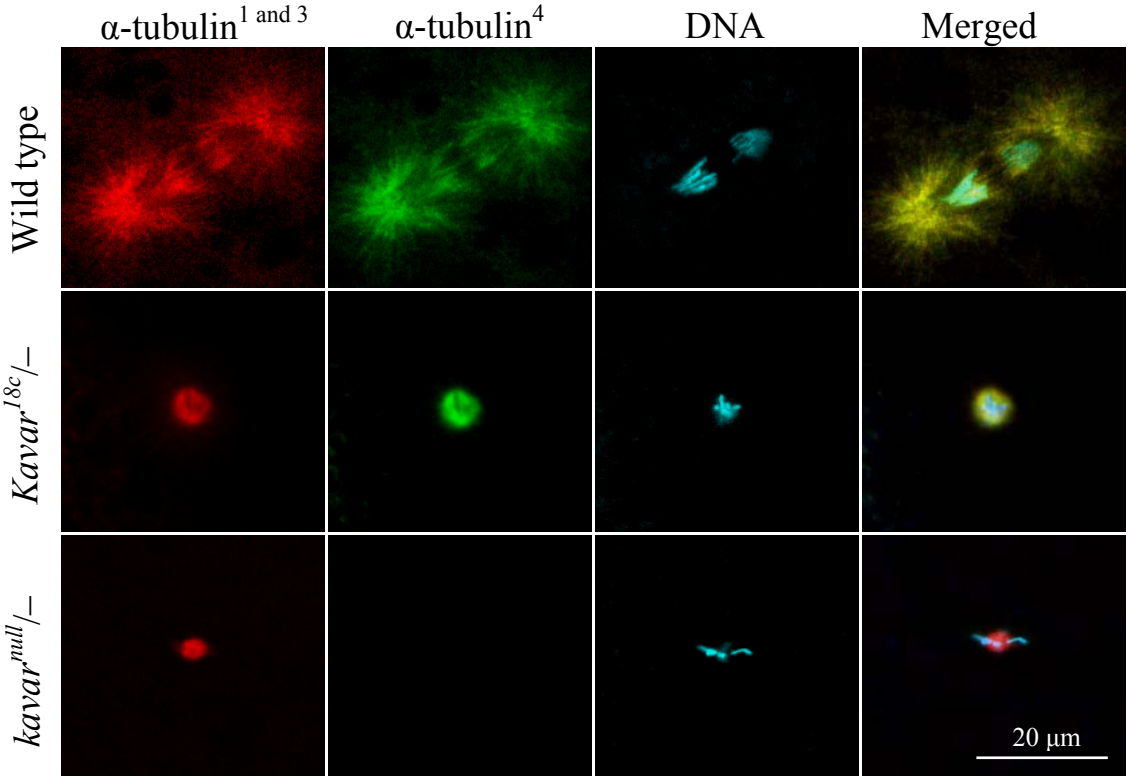

Figure 10. Localization of α-tubulin[1and 3], α-tubulin[4] and DNA in the first mitotic spindle of embryos of wild type, *Kavar*^{18c}/– and *kavar*^{null}/– females. The first and only spindle which appears in eggs of the mutant females appears as a tassel of short MTs in eggs of the *Kavar*^{18c}/– and *kavar*^{null}/– females.

Ectopic expression of E82K-α-tubulin[4]

As mentioned in the cytoplasm injection section, the injected *Kavar*^{18c}/– egg cytoplasm, with E82K-α-tubulin[4] inside, did not do any harm to those embryos that accomplished the 12[th] cleavage division. To clarify the effect of E82K-α-tubulin[4] we constructed UAS-*Kavar*^{18} (and, as control, UAS-*α-tubulin67C*) transgenes and expressed the transgenes by different tissue specific *Gal4* drivers (Table 5). We presumed that the ectopically expressed E82K-α-tubulin[4] can bring about cell death and the *Gal4*; UAS-*Kavar*^{18} combination will not survive to adulthood or possess developmental abnormalities. For example, the *ey-Gal4*; UAS-*Kavar*^{18} flies (in which the eye disc specific *ey-Gal4* driver leads to production of E82K-α-tubulin[4] in the eye imaginal disc cells) were expected not to have eyes. We selected a set of *Gal4* drivers that ensured the production of E82K-α-tubulin[4] in basically all the different cell types (Table

5). In all the crosses the *Gal4*; UAS-*Kavar*^{18} zygotes developed to adult at the expected proportion and without any delay and here was no indication of cell death or developmental abnormality (Table 5). The *α-tubulin84B-Gal4* driver – in which *Gal4* is produced under promoter of the constitutively expressed *α-tubulin84B* gene (Lee and Lou 1999) - ensures production of E82K-α-tubulin^4 in all the cells and yet the *α-tubulin84B-Gal4*; UAS-*Kavar*^{18} zygotes are fully viable. The above result clearly shows that ectopic expression of E82K-α-tubulin^4 does not reduce cell viability. Ectopic expression of the normal UAS-*αTub67C* gene (in *Gal4*; UAS-*αTub67C* zygotes) did not alter normal development in all the *Gal4* drivers listed in Table 5.

Table 5. Features of the *Gal4*; *UAS-Kavar*^{18c} combinations

Gal4 driver	Expression pattern	Feature of the *Gal4*; *UAS-Kavar*^{18c} combination
distalless	diploid cells	Fully viable
elav	nervous system	Fully viable
engrailed	epidermis, central nervous system	Fully viable
escargo	diploid cells	Fully viable
eyeless	central nervous system, eye-antennal disc	Fully viable
nanos	female germ-line	Females sterile
patched	adult sternite	Fully viable
scabrous	nervous system, epidermis	Fully viable
twist	mesoderm, ectoderm	Fully viable
vestigal	diploid cells	Fully viable
α-tubulin84B	Ubiquitous	Females sterile

To see whether the ectopically expressed E82K-α-tubulin^4 (also the normal E82K-α-tubulin^4) molecules are incorporated into the MTs and whether they affect length of the MTs we generated *elav-Gal4*; UAS-*Kavar*^{18} (and control *elav-Gal4*; UAS-*α-tubulin67C*) larvae dissected the ventral ganglia and analyzed the neuroblast cells. As shown on Figure 11, the E82K-α-tubulin^4 as well as the α-tubulin^4 molecules become incorporated into the spindle apparatus and do not alter its shape or size. The longest MTs are 6-8 μm and are apparently fully functional implying non toxic effect of E82K-α-tubulin^4 on the MT system of the cells.

It should be mentioned that the lack of zygotic death or abnormal development is certainly not the consequence of non-functional UAS-*Kavar*^{18} transgene since when driven by the female germ line specific *nanos-Gal4* or the all-over *α-tubulin84B-Gal4* driver the females are sterile and their embryos showed defects described for the embryos of *Kavar*^{18c}/+ females.

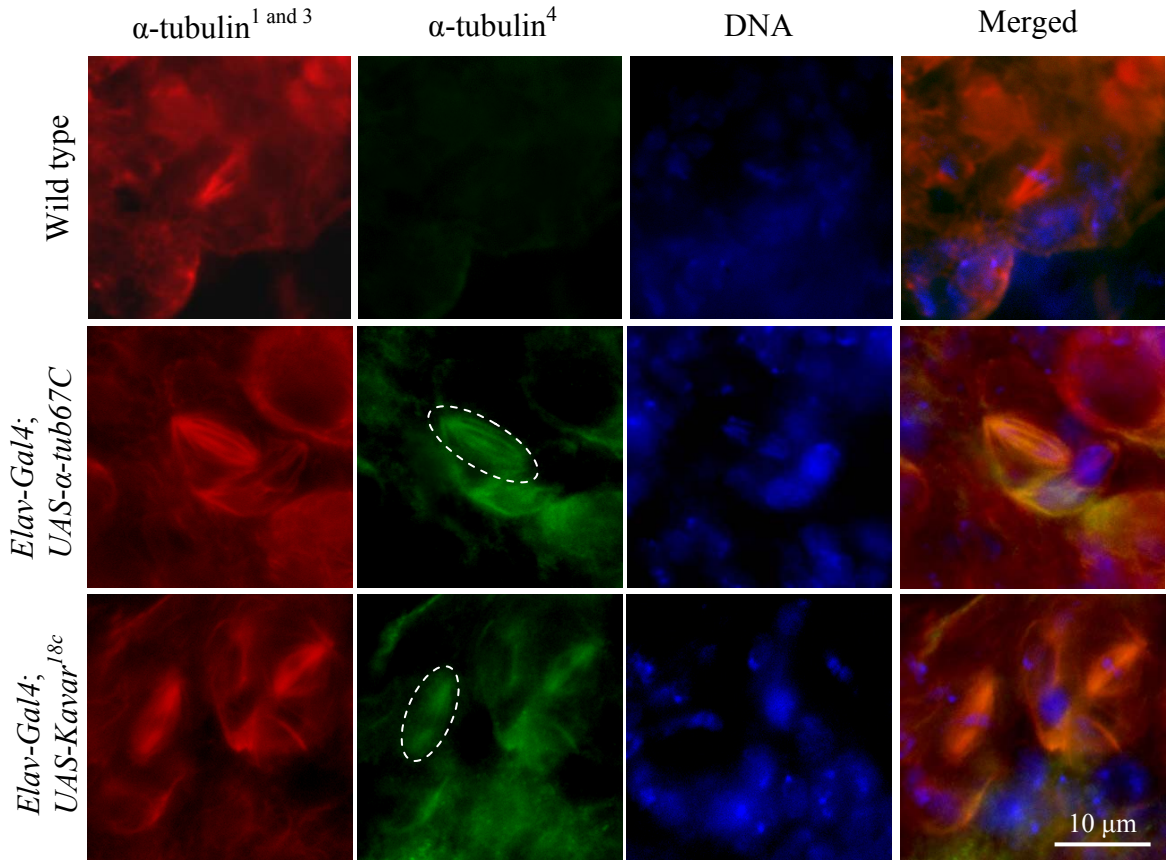

Figure 11. The ectopically expressed α-tubulin[4] and E82K-α-tubulin[4] molecules become incorporated into the MTs in the neuroblast cells as shown by the encircled spindle apparatus. α-tubulin[1] and α-tubulin[3] were detected by the monoclonal DM1A primary and a red fluorescing, α-tubulin[4] and E82K-α-tubulin[4] by a polyclonal primary anti-α-tubulin[4] and a green fluorescing secondary antibody. Ectopic expression of α-tubulin[4] and E82K-α-tubulin[4] was achieved by driving *UAS-α-tubulin67C* and *UAS-Kavar*^{18c} transgenes with the nervous system specific *elav-Gal4* driver.

Effect of wild type and E82K α-tubulin[4] on *in vitro* polymerized MTs

To determine the role of α-tubulin[4] in MT formation and how E82K-α-tubulin[4] exerts its toxic effect we carried out two sets of *in vitro* MT polymerization assays. We prepared extracts from eggs of +/– (control), *Kavar*^{18c}/– and *kavar*^{null}/– females and induced tubulin polymerization in the presence and also in the absence of taxol. The results are summarized in Table 6. While in absence of taxol only nucleation seeds and no MTs form in extract of the *Kavar*^{18c}/– females, MTs do form - though shorter than in the control (4.6 versus 9.9; $P<0.01$) - in the presence of taxol, a MT stabilizing agent, showing that taxol partially compensate the MT destabilizing action of E82K-α-tubulin[4].

Table 6. Length of the MTs which form during in vitro tubulin polymerization

Type of in vitro tubulin polymerization assay[1]	Genotype of females[2]	Length of the forming MTs (μm)			
		Average	± SD	n	Min. and max.
From embryo extract in presence of taxol. 37ºC, 30 min	+/– (Control)	9.9	5.2	375	2.4 and 41.6
	Kavar^{18c}/–	4.6*	2.4	227	1.1 and 16.7
	kavar^{null}/–	7.0*	4.0	303	2.0 and 28.7
From embryo extract in absence of taxol. 37ºC, 30 min	+/– (Control)	11.5	4.0	887	3.6 and 28.8
	Kavar^{18c}/–	Only nucleation seeds form			
	kavar^{null}/–	11.7	5.2	534	1.4 and 29.1

[1] The MTs were made visible by incorporation of bovine tubulin that was fluorescently labeled by Oregon-green 514.
[2] The females were collected as virgins and were than mated with X0 males to stimulate egg production. Egg extracts were prepared from their eggs.
* Significantly different from the control ($P<0.01$; one-way ANOVA)

Unexpectedly, the MTs grew to basically equal size in egg extract of the control (+/–) and the *kavar*^{null}/– females (11.5 versus 11.7; Table 6). It appears that equally long MTs form if sufficiently long time is available for tubulin polymerization, irrespectively from the presence or absence of α-tubulin^{4}. The result implies that α-tubulin^{4} is required for rapid tubulin polymerization and not per se for the formation of lengthy MTS. To test the effect of α-tubulin^{4} on MT polymerization we studied the kinetics of tubulin polymerization in egg extracts of virgin +/– and *kavar*^{null}/– females, i.e. determined length distribution of the forming MTs versus the time allowed for tubulin polymerization. As Figure 12 shows, there is a remarkable difference in kinetics of MT formation in the two types of egg extracts. While MTs with measurable length appear after five minutes in the control, only nucleation seeds form in the *kavar*^{null}/– egg extract. During early phase of elongation even the longest MTs that form in absence α-tubulin^{4} are shorter than most of the MTs that form in presence of α-tubulin^{4} (Figure 12). Analysis of polymerization kinetics revealed very similar average MT growth speeds (Figure 13; the maximum of 0.35 μm/min in the control and 0.32 μm/min in the null). However, while in the control preparations the maximum speed is reached by 15 minutes it took 25 minutes in absence of α-tubulin^{4} (Figure 13). It seems that α-tubulin^{4} accelerates MT formation and thus α-tubulin^{4} is required for rapid tubulin polymerization.

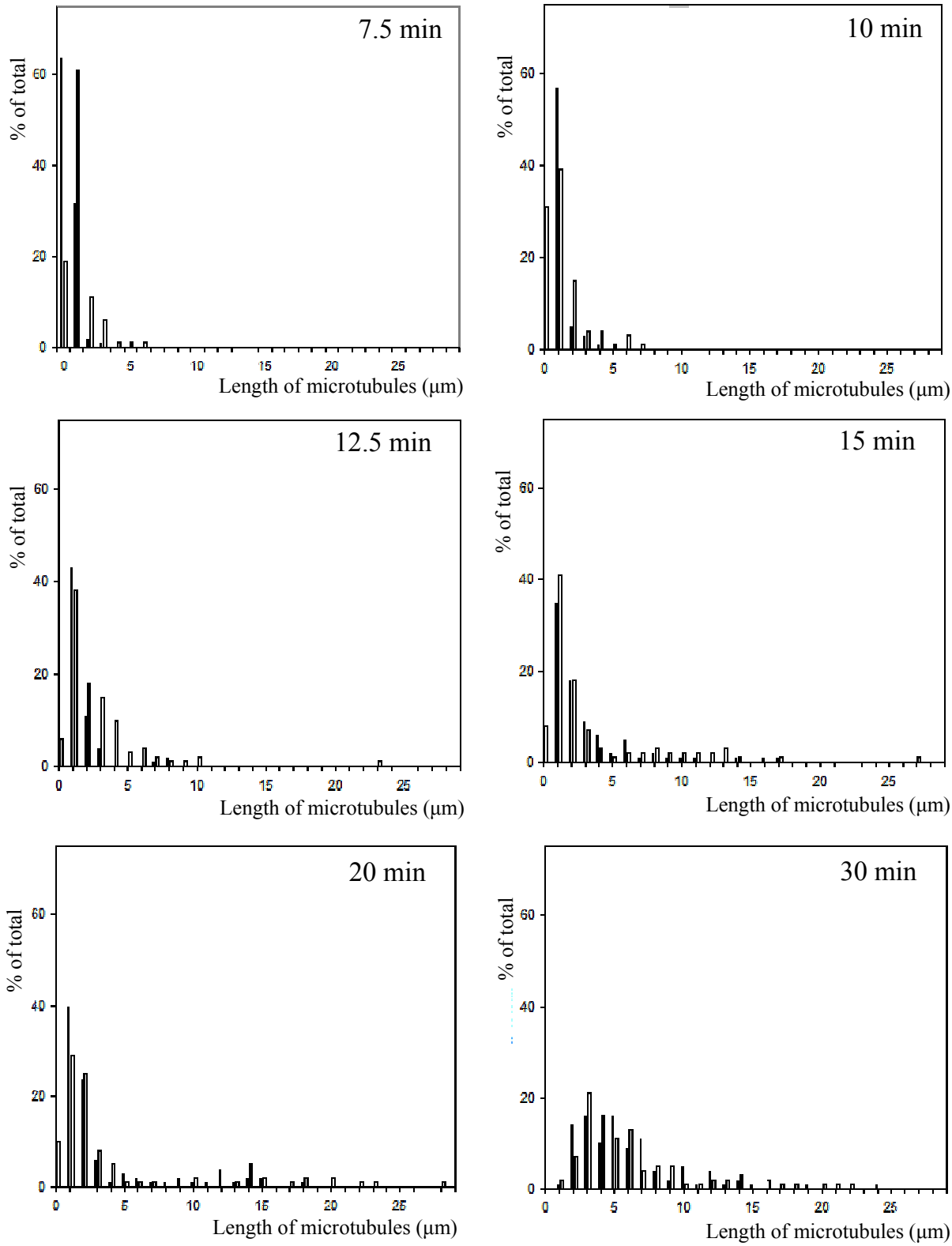

Figure 12. Length distribution of the microtubules that form during *in vitro* tubulin polymerization in extract of virgin control (+/–) and *kavar*^{0}/– females following different amount of time. The 0 class represents nucleation seeds that do not reach 1 µm in length.

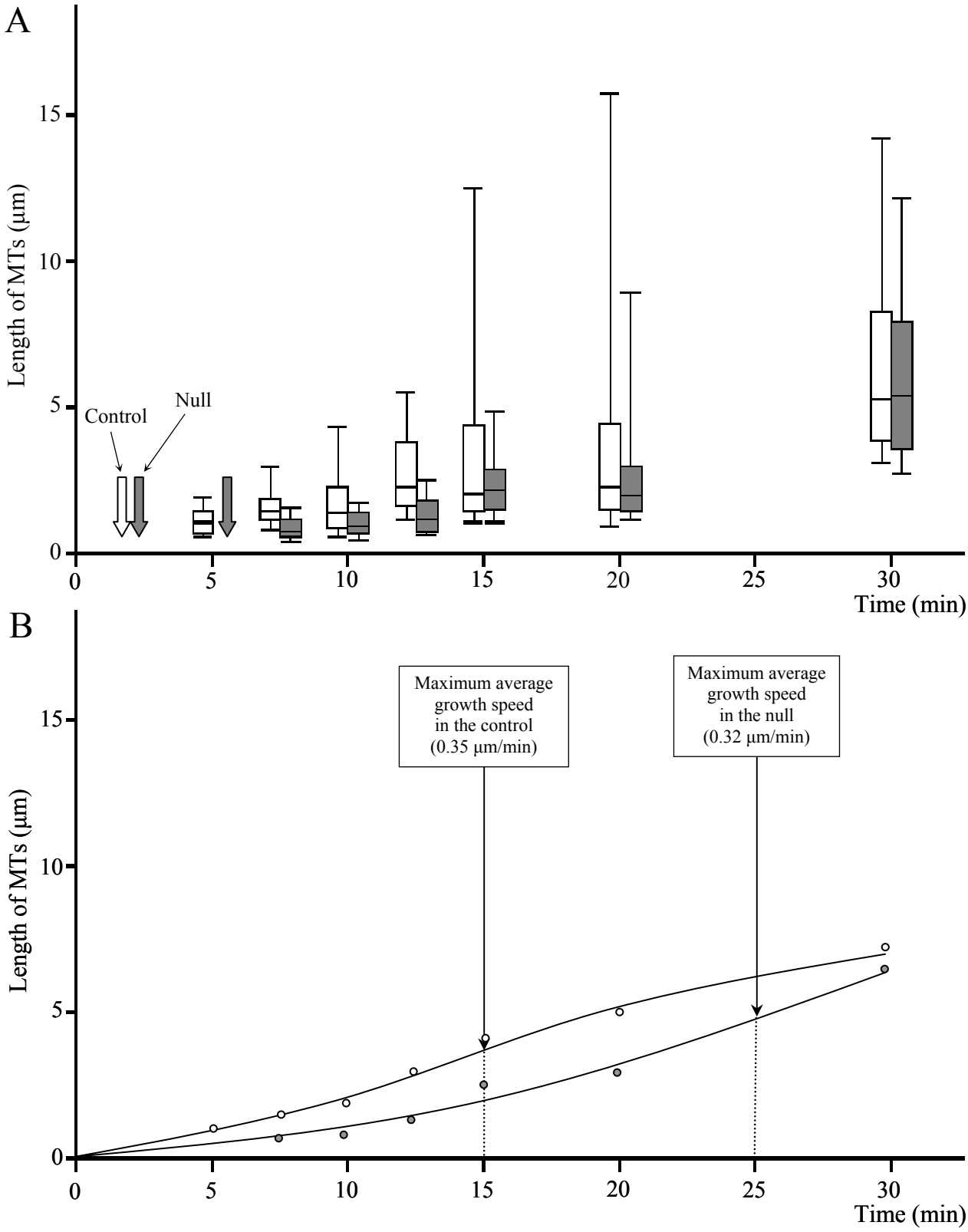

Figure 13. The kinetics of tubulin polymerization *in vitro*. Length distribution of the forming MTs plotted against time. (A) White and grey arrows and bars correspond to egg extracts of females with one normal *αTub67C* gene (+/– as control) and eggs of females that did not carry functional *αTub67C* gene ($kavar^{null}$/–), respectively. The wide arrows represent preparations in which only nucleation seeds appeared. The five horizontal lines in the box plots correspond to 10th, 25th, 50th, 75th and 90th percentiles, respectively. (B) White and grey points represent average MT lengths for the control (+/–) and for the null ($kavar^{null}$/–) conditions.

DISCUSSION

Mapping the *Kavar^D* and the *kavar^r* alleles

The *αTub67C* gene has been identified previously by partial loss-of-function (the *αTub67C$^-$* mutations; Matthews *et al.*1993), by the *Tomaj^D* dominant female-sterile mutations and their *tomaj^r* revertant alleles (Máthé *et al.* 1998) and also by a P-element induced semi-dominant allele (Matthies *et al.* 1999). We describe here that the *Kavar^D* mutations and their *kavar^r* revertant alleles identify the *αTub67C* gene. Although the *Fs* mutations were mapped and complementation analyses were conducted with selected revertant alleles of those *Fs* mutations that either map into the same chromosome interval or possess very similar mutant phenotype (Erdélyi and Szabad 1989), allelism of the *kavar^r* and the *tomaj^r* alleles went undetected. There are three excuses to explain the oversight. (1) The remarkable difference between the *Kavar^D* and the *Tomaj^D* mutant phenotypes. (2) Inaccuracy in mapping of the dominant female-sterile mutations on the basis of mitotic recombination induced in the female germ line (Erdélyi and Szabad 1989). (3) A misfortune in choosing *kavar^{re21}* (which turned out to be a recombinant chromosome; Table 1) to represent *Kavar^{21g}* in the complementation analyses. In any case the *Kavar^D* and the *kavar^r* alleles identify the *αTub67C* gene (Venkei and Szabad 2005).

The *Kavar^D* dominant negative mutations reveal novel functions of α-tubulin^4

It was shown earlier that the *αTub67C* gene is expressed in the female germ line during oogenesis and the encoded so-called maternal α-tubulin^4 is a component of the MTs in the oocyte and in the early embryo (Kalfayan and Wensink 1982; Mischke and Pardue 1982; Matthews *et al.* 1989; Theurkauf *et al.* 1986; Theurkauf 1992). The previously described partial loss-of-function and the gain-of-function mutations in the *αTub67C* gene showed involvement of the encoded α-tubulin^4 in meiosis, cleavage mitoses, formation of the sperm aster and the embryonic central as well as the peripheral nervous systems (Theurkauf 1992; Matthews *et al.*1993; Máthé *et al.* 1998; Matthies *et al.* 1999). The *Kavar^D* dominant negative mutations revealed formerly not reported function of α-tubulin^4 in formation of the cleavage spindles (Venkei and Szabad, 2005; Venkei *et al*., 2006). While the *Kavar^{18c}* encoded E82K molecules bring about their deleterious effects at the commencement of embryogenesis, action of the *Kavar^{21g}* encoded E426K molecule is less severe and may be manifested as late as migration of the cleavage nuclei into the egg cortex.

The failure of proper separation of the daughter centrosomes in the derived "die at start" embryos of both the *Kavar*^{18c}/+ and the *kavar*^{null}/– females has not been reported earlier and revealed novel function of α-tubulin^4. Interestingly, although the E82K α-tubulin^4 molecules are present throughout oogenesis in egg primordia of the *Kavar*^{18c}/– females there is no sign of toxic activity of the encoded E82K α-tubulin^4. Similarly, the lack of α-tubulin^4 throughout embryogenesis has no consequences on oogenesis, implying that the α-tubulin^4 molecules that are encoded by the *αTub67C*$^-$ (Matthews *et al.*1993) and by the P-element induced allele *αTub67C*^{P40} (Matthies *et al.* 1999) exert their deleterious action by becoming activated already during oogenesis where - as shown by normal progression of oogenesis in the *kavar*^{null}/– females - function of α-tubulin^4 is not required.

The lack of α-tubulin^4 or the toxic effect of E82K-α-tubulin^4 is manifested at the onset of embryogenesis and appears as a failure of appropriate separation of the daughter centrosomes. The fact, that the lack of α-tubulin^4 and the defect caused by E82K-α-tubulin^4 have identical consequences suggests that *Kavar*^{18c} identify an isoform specific function. Indeed, *Kavar*^{18c} is a dominant negative mutant allele since extra *αTub67C* gene - in *Kavar*^{18c}/+/+ females - slightly rescues the *Kavar*^{18c} mutant phenotype.

Requirement of α-tubulin^4 in daughter centrosome separation

Non-separated centrosomes, which appear in embryos of the *Kavar*^{18c}/+ and the *kavar*^{null}/– females, can form through two mechanisms: due to failure of the daughter centrosomes to separate in interphase (Robinson *et al.*, 1999), or spindle collapse (Sharp *et al.* 1999). Spindle maintenance and elongation during mitosis is based on change in balance between opposing forces exerted on the antiparallel MTs in the spindles by KLP61F and the Non-claret-disjunctional motors (Sharp *et al.*, 1999; Scholey *et al*,. 2003). Through which of the mechanisms do monopolar spindles originate in eggs of the *Kavar*^{18c}/+ and the *kavar*^{null}/– females? The answer came from real-time imaging of live embryos into which cytoplasm from eggs (with E82K-α-tubulin^4 in it) of *Kavar*^{18c}/– females were injected. Since the mutant cytoplasm did not cause any harm when injected during meta- or anaphase, we concluded that α-tubulin^4 is not required for maintenance and elongation of the spindle apparatus but rather for separation of the daughter centrosomes during inter- and early prophase.

The mechanism of daughter centrosome separation

In wild type Drosophila embryos the centrosomes replicate during telophase, a process that leads to the formation of two daughter centrosomes (Foe *et al.* 1993; Sullivan and Theurkauf

1995; Debec *et al.* 1999). The daughter centrosomes move apart along the nuclear envelope during the subsequent interphase and prophase. Once in the egg cortex, (i.e. in embryos beyond the 10th cleavage cycle) the daughter centrosomes are separated by two mechanisms (Cytrynbaum *et al.*, 2003). The pushing force generated by the growing MTs that encounter the other centrosome. Assuming radial array of the MTs – that are nucleated by the centrosomes - the polymerization force decreases exponentially and becomes ineffective by about 2-3 μm for two reasons: (i) the number of MTs encountering the other centrosome drops off with increase of the separation distance and (ii) the receding centrosomes disappear on the nuclear horizon (Figures 14 and 15). In the egg cortex the task of centrosome separation is taken over from the growing and pushing MTs by cytoplasmic dynein that is associated with the subcortical actin network (Figure 14; Scholey et al., 2003; Cytrynbaum et al., 2003; Cytrynbaum et al., 2005). The outward forces, which separate now the daughter centrosomes are compensated by the inward force generated by the C-terminal kinesin Ncd, and the final result depends on shift in a balance between the inward and the outward forces (Figure 14; Robinson et. al 1999; Sharp *et al.* 2000a and 2000b; Scholey *et al.* 2003; Cytrynbaum *et al.* 2003; Cytrynbaum et al., 2005).

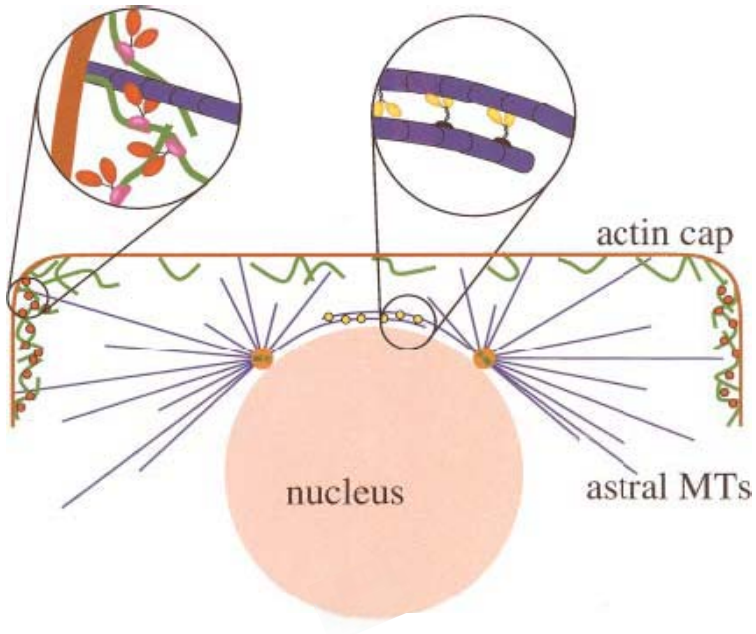

Figure 14. Components involved in centrosome separation in cleavage nuclei in the egg cortex. The nucleus (pink disc) is relatively isolated from the neighbor nuclei by the surrounding furrows (brown curve). The actin cap binds - through dynactin - to dynein. MTs extend outward from each of two daughter centrosomes. The C-terminal kinesin - Ncd – binds to the antiparallel MTs. After Cytrynbaum *et al.* 2003.

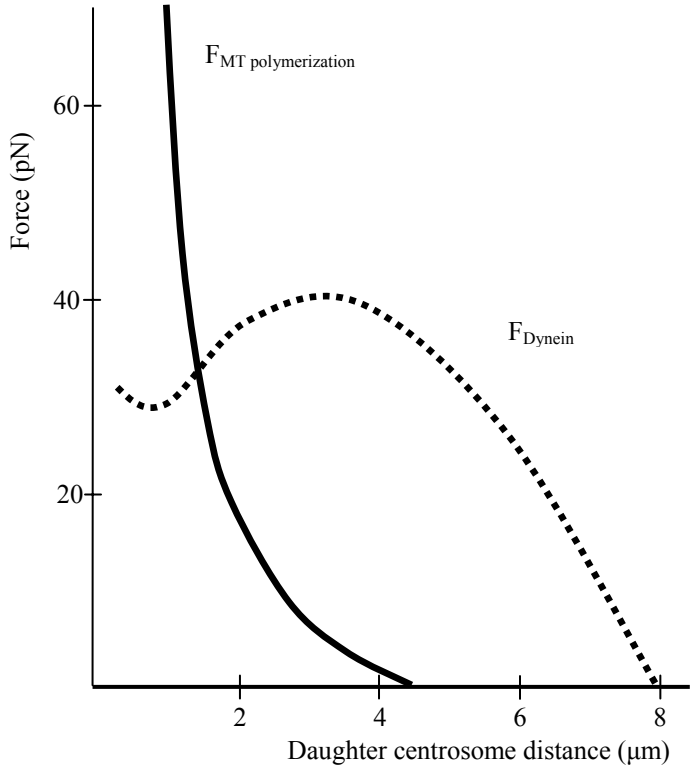

Figure 15. Forces - that act to separate the daughter centrosomes - as a function of distance between the centrosomes during interphase of the 12th cleavage division. The calculated forces that are generated by dynein (F_{Dynein}) and by polymerization ($F_{MT\ polymerization}$) in the wild-type embryo are plotted (after Cytrynbaum *et al.* 2003).

The situation is different deep inside the egg cytoplasm since the cytoplasmic dynein associated with the subcortical actin network can not participate in separation of the daughter centrosomes. There must be another mechanism operating and achieving proper centrosome separation. We propose that long MTs, including the interpolar MTs, and cytoplasmic dynein hooked to the nuclear envelope and migrating along the MTs in vicinity of the nuclear envelope participate in centrosome separation (see below). In any case, to function properly, the interpolar MTs need to meet three requirements.

(i) They must be able to follow the curvature of the nuclear envelope. Indeed, as we described, the α-tubulin[4] is enriched in the interpolar microtubules, a phenomenon not observed in absence of α-tubulin[4] (Venkei *et al.* 2006). The mechanism that ensures contact between the interpolar MTs and the nuclear envelope remains to be solved. Large nuclei with mild curvature are expected to be more appropriate for the interpolar microtubules to follow

than the small nuclei around which the microtubules may simply break. In fact nuclei with about 10 μm diameter are characteristic up to the 9th cleavage cycle that allow the formation of 15-16 μm long interpolar MTs (Figure 16). It may be a sacrilege to propose that the early cleavage nuclei are kept large (with small curvature) such that while growing and pushing the daughter centrosomes apart the interpolar microtubules can bend along the nuclear envelope. Once the nuclei reach to the egg cortex and cytoplasmic dynein that is associated with the subcortical actin network joins in the task of centrosome separation the microtubules need not grow too long anymore and the embryos can afford to have small nuclei.

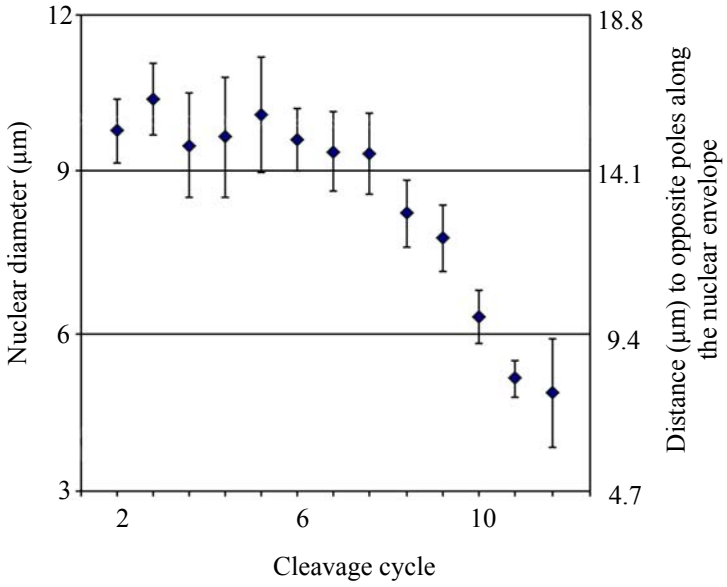

Figure 16. Diameter of the cleavage nuclei in late interphase throughout the cleavage cycles in *Drosophila melanogaster* embryos. Nuclear diameters were measured following DAPI staining of (at least ten embryos and about 20 nuclei) fixed embryos. The distance to opposite poles along the nuclear envelope was calculated by assuming ball shaped nuclei.

(ii) The interpolar microtubules must grow long to be able to reach over to opposite poles of the early cleavage nuclei. Indeed, in absence of α-tubulin^4 only short MTs form.

(iii) The interpolar microtubules need to grow fast. The conclusion, i.e. α-tubulin^4 is required for the formation of lengthy MTs, is superficial. *In vitro* polymerization of tubulins revealed that once sufficiently long time is available for polymerization equally long MTs form whether α-tubulin^4 is present or absent and thus it is safe to conclude that α-tubulin^4 is required for rapid formation of long MTs (Figure 12 and 13). It appears that although tubulin polymerization starts in eggs of the *kavar*^{null}/– females it proceed too slow and thus the forming MTs can not grow sufficiently lengthy within the time available for the process. The time allowed for tubulin polymerization is limited by the CyclinB/Cdc2 controlled cyclic sets of events which start during egg activation, whether the egg is fertilized or not (Edgar and Datar 1996; Donaldson et al., 2001; Ji et al., 2004; Tadros and Lipshitz 2005). In fact, since

diameter of the nuclei is about 10 μm up to the 9th cleavage cycle, the interpolar MTs need to be as long as 15-16 μm concerning perfect geometrical parameters during interphase (Figure 16). Since duration of an early cleavage cycle is about 8 min of which the interphase comprises about 4 min (Foe et al., 1993; Ji et al. 2004), the interpolar MTs must grow "fast" (with a speed of about 4 μm/min) to fulfill their functions. Along progression beyond the 9th cleavage cycle size of the nuclei decreases to about 5 μm and correspondingly the interpolar MTs need to grow only about 8 μm long to extend over the opposite poles and since length of the interphase in cleavage cycle 10 is about 6 min (Ji et al. 2004), the "slow" MT growth rate of 1.3 μm/min may be adequate for the formation of sufficiently long interpolar MTs. The lack of formation of sufficiently long MTs leads to arrest of the cleavage cycles and death of the embryos. Similar "out of phase" and "behind schedule and lost" types of events have been reported during Drosophila embryogenesis. For example, in embryos defective in cytoplasmic dynein heavy chain function the replication cycle comes to an end soon after fertilization while the centrosome cycles proceed normally (Belecz et al., 2001).

Concerning features of α-tubulin[4] we propose the following model for the separation of the daughter centrosomes in the early cleavage embryos (Figure 17). Some of the forming MTs - the interpolar MTs - emanating from the centrosomes exert mutual pushing force on the daughter centrosomes. The pushing force is highest when the daughter centrosomes are in close vicinity and several of the growing MTs hit the centrosomes. The interpolar MTs push the daughter centrosomes apart while they grow along the surface of the nuclear envelope.

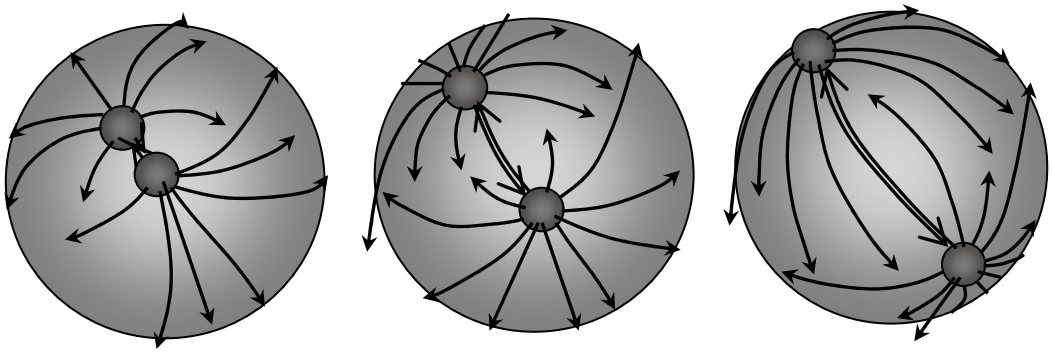

Figure 17. Simplified model to explain the mechanism of daughter centrosome separation and migration in the early cleavage (cycles 2 - 9) Drosophila embryos. The interpolar microtubules, nucleated by the daughter centrosomes (labeled by large arrowheads) exert pushing force and begin to separate the daughter centrosomes. The α-tubulin[4] containing microtubules bend around the nuclear envelope while they grow. Dyneins hooked to the nuclear envelope (not shown on the model) keep the microtubules attached and use those as a migration route to pull the centrosomes in the indicated directions. Centrosome migration stops when the interpolar microtubules bend away from the nuclear envelope and the centrosomes organize symmetric array of microtubules equalizing inward and outward forces.

Centrosomes stop separating once they are about 160 degree apart and the interpolar MTs depart from the nuclear envelope (Robinson et al., 1999; Cytrynbaum et al., 2003). It well may be that the cytoplasmic dynein molecules, that establish contact between the nuclear envelope and the nearby MTs (Reinsch and Gönczy, 1998; Robinson et al. 1999), are also involved in separation of the daughter centrosomes. Involvement of cytoplasmic dynein in maintenance of connection between the nuclear envelope and the nearby MTs is elegantly shown by the finding that in embryos of *Laborc*^{17c} females - with mutant cytoplasmic dynein in their egg cytoplasm - the centrosomes detach from the nuclear envelope (Belecz et al., 2001).

At the beginning of daughter centrosome separation the centrosomes organize asymmetric array of MTs that are in contact with the nuclear envelope (Figure 17). (A similar condition was recently suggested for the astral MTs by Cytrynbaum et al. 2005). While dyneins - hooked to the nuclear envelope - move along the nearby MTs they pull the daughter centrosomes apart. Contribution of dynein to centrosome separation ceases by the time when the centrosomes are distantly located and nucleate symmetrical arrays of MTs (Figure 17).

There seems to be no well-defined trail for migration of the centrosomes along the nuclear envelope since orientation of at least the first cleavage spindle - that is organized by the pushed apart daughter centrosomes - is random. Random orientation of the first cleavage spindle has been long known from random orientation of the XX/X0, female/male borderline in gynandromorphs (Janning, 1978).

Why is E82K-α-tubulin^4 non toxic on late cleavage embryos and cells

E82K-α-tubulin^4, that is very toxic to the early cleavage embryos, is harmless to late cleavage embryos and does not disturb MT functions in the dividing cells. Explanation of the unexpected behavior of E82K-α-tubulin^4 is most likely related to a major difference between the early and the late cleavage cycles and the dividing cells. As discussed above, during the last cleavage divisions in the egg cortex the forming MTs are long enough to push the daughter centrosomes to some 2-4 μm apart, to a distance where cytoplasmic dynein - anchored to the cortical actin network or to the cell membrane - takes over the task of centrosome separation from the growing MTs. Cytoplasmic dynein generate the pulling force required for separation of the daughter centrosomes (Figure 14; Robinson et al., 1999; Sharp et al., 2000a and 2000b; Scholey et al., 2003; Cytrynbaum et al., 2003). Although the E82K-

α-tubulin^4 containing MTs grow shorter than normal, they are long enough to "hand over" the daughter centrosomes to cytoplasmic dynein that will carry on and accomplish centrosome separation. The situation is very similar in the imaginal disc and in the neuroblast cells where incorporation of E82K-α-tubulin^4 into the MTs has no apparent consequences.

The mode of normal and E82K-α-tubulin^4 action

Complete loss of *αTub67C* gene function (in eggs of the *kavar^{null}*/– hemizygous females) revealed that α-tubulin^4 is required for the rapid formation of lengthy MTs. Although the α-tubulin^4 molecules comprise only about 20% of the α-tubulin pool in the Drosophila eggs (Matthews *et al.*1989) only 2-3 μm MTs form in absence of α-tubulin^4. How can incorporation of one isotype lead to rapid polymerization of elongated MTs? What makes α-tubulin^4 special? Although we have no experimental data to answer the former questions, α-tubulin^4 is a rather divergent type of the four Drosophila α-tubulins. It shares a 68% (315/452) amino acid identity with the evolutionary highly conserved α-tubulin^1 and α-tubulin^3 isoforms (Figure 18). The sequence divergence spreads basically all over its range. Sequence analysis showed that the most characteristic part of the primary structure is the insertion of an 11 amino acid blocks between position 51 and 52, in the GTP binding domain that has been known to be responsible inside the polymer tube for the intra- and intermolecular connections: for tubulin and MT stability (Nogales, 1999).

How does E82K-α-tubulin^4 exert its toxic effect? The 82nd Glu$^-$ (that is Glu^{71} in bovine α-tubulin, see Figure 18) is an important component of the conserved non-exchangeable GTP binding site and is responsible for binding of a Mg^{2+} that is engaged - along with a number of amino acid side chains - in binding GTP, a structural component of the α-tubulins (Figure 19; Löwe *et al.*, 2001). The E82K-α-tubulin^4 molecules, in which Glu^{82} was replaced by Lys$^+$, become incorporated into the MTs however they render the MTs unstable (see Figure 9 and Table 6).

We conclude, based on the data presented in this Ph.D. thesis and in the accompanying papers, that α-tubulin^4 is a tool of the Drosophila mothers to ensure appropriate embryogenesis of their progeny: α-tubulin^4 is required for the fast formation of interpolar microtubules to push the daughter centrosomes to opposite poles, a precondition for setting spindle apparatus, to accomplish the initial cleavage divisions.

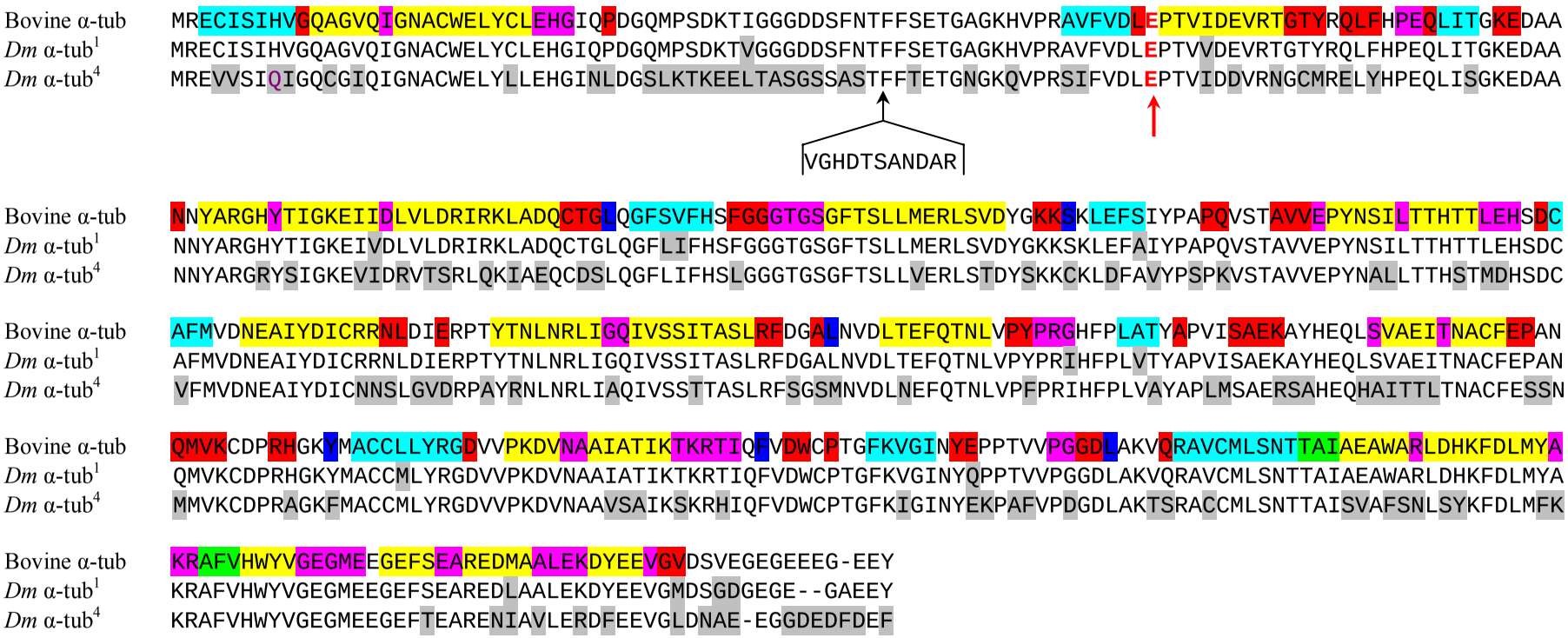

Figure 18. Amino acid sequence of bovine α-tubulin and two Drosophila α-tubulins: the constitutively expressed α-tubulin[1] (that differs only in two amino acids from α-tubulin[3]) and α-tubulin[4], the so-called maternal isotype. (See SwissPort http://www.expasy.org/sprot). The differences between bovine and Drosophila α-tubulin[1] appear as shaded letters in the α-tubulin[1], the differences between α-tubulin[1] and α-tubulin[4] appear as shaded letters in α-tubulin[4] sequence. The assignments in the bovine α-tubulin are as follows: yellow = helix; blue = residue in isolated beta bridge; turquoise = extended β strand; green = 310 helix type; purple = hydrogen bonded turn; red = bend. Position of E (that is K in the *Kavar*^{18c}-encoded E82K-α-tubulin[4]) is labeled by a red arrow.

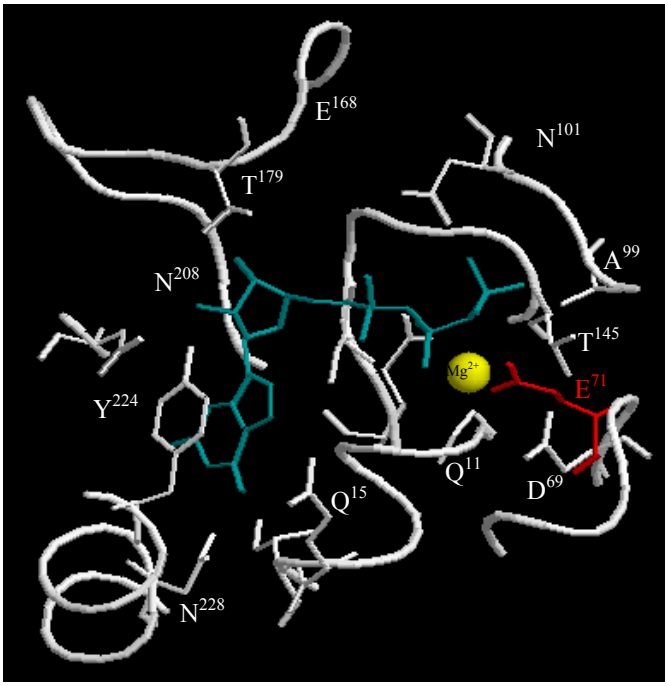

Figure 19. The GTP-binding moiety in an α-tubulin molecule. The GTP appears in blue, E^{71} (that is E^{82} in α-tubulin[4]) is highlighted in red and the Mg^{2+} appears in yellow. (After Löwe *et al.* 2001; (http://www.rcsb.org/pdb/).

REFERENCES

Adams MD, Celniker SE, Holt RA, Evans CA, Gocayne JD (2000) The genome sequence of *Drosophila melanogaster*. Science 287, 2185-2195.

Alberts B, Bray D, Lewis J (1994) Molecular Biology of the Cell. 3rd ed. Garland Publishing, Inc., New York, London.

Belecz I, Gonzalez C, Puro J and Szabad J. (2001) Dominant-negative mutant dynein allows spontaneous centrosome assembly, uncouples chromosome and centrosome cycles. Curr. Bio.l 11, 136-140.

Bhattacharya R, Cabral F (2004) A ubiquitous beta-tubulin disrupts MT assembly and inhibits cell proliferation. Mol. Biol. Cell. 15, 3123-3131.

Bode CJ, Gupta ML, Suprenant KA, Himes RH. (2003) The two alpha-tubulin isotypes in budding yeast have opposing effects on MT dynamics *in vitro*. EMBO Rep. 1, 94-99.

Brust-Mascher I, Civelekoglu-Scholey G, Kwon M, Mogilner A, Scholey JM (2004) Model for anaphase B: role of three mitotic motors in a switch from poleward flux to spindle elongation. Proc Natl Acad Sci USA. 101, 15938-15943.

Cassimeris L (1993) Regulation of MT dynamic instability. Cell Motil Cytoskeleton. 26, 275-81.

Clarkson M., Saint R. (1999) A His2AvDGFP fusion gene complements a lethal His2AvD mutant allele and provides an in vivo marker for Drosophila chromosome behavior. DNA Cell Biol. 18, 457-462.

Cullen CF, Deak P, Glover DM, Ohkura H (1999) mini spindles: A gene encoding a conserved MT-associated protein required for the integrity of the mitotic spindle in Drosophila. J Cell Biol. 146, 1005-1018.

Cytrynbaum EN., Scholey JM., Mogilner A. (2003) A force balance model of early spindle pole separation in Drosophila embryos. Biophys J. 84, 757-769.

Cytrynbaum EN., Sommi P., Brust-Mascher I., Scholey JM., Mogilner A. (2005) Early spindle assembly in *drosophila* embryos: role of a force balance involving cytoskeletal dynamics and nuclear mechanics. Molecular Biology of the Cell 16, 4967–4981.

Deák P, Omar MM, Saunders RDC, Pal M, Komonyi O, Szidonya J, Maróy P, Zhang Y, Ashburner M, Benos P, Savakis C, SidenKiamos I, Louis C, Bolshakov VN, Kafatos FC, Madueno E, Modolell J, Glover DM (1997) P-element insertion alleles of essential genes on the third chromosome of *Drosophila melanogaster*: Correlation of physical and cytogenetic maps in chromosomal region 86E-87F. Genetics 147, 1697-1722

DeRenzo C, Seydoux G (2004) A clean start: degradation of maternal proteins at the oocyte-to-embryo transition. Trends Cell Biol. 14, 420-426.

Debec A, Marcaillou C, Bobinnec Y, Borot C (1999). The centrosome cycle in syncytial Drosophila embryos analyzed by energy filtering transmission electron microscopy. Biology of the Cell 91, 379-391.

Dettman RW, Turner FR, Hoyle HD, Raff EC (2001) Embryonic expression of the divergent Drosophila beta3-tubulin isoform is required for larval behavior. Genetics. 1, 253-263.

Dogterom M, Kerssemakers JW, Romet-Lemonne G, Janson ME (2005) Force generation by dynamic MTs. Curr Opin Cell Biol. 17, 67-74.

Downing KH, Nogales E (1998) Tubulin structure: insights into MT properties and functions. Curr Opin Struct Biol. 8, 785-791.

Duffy JB (2002) GAL4 system in Drosophila: a fly geneticist's Swiss army knife. Genesis. 34, 1-15.

Dutcher SK (2001) The tubulin fraternity: alpha to beta. Curr Opin Cell Biol. 13, 49-54.

Edgar BA and Datar SA (1996) Zygotic degradation of two maternal Cdc25 mRNAs terminates Drosophila's early cell cycle program. Genes Dev. 10, 1966-1977.

Erdélyi M, Szabad J (1989) Isolation and characterization of dominant female sterile mutations of *Drosophila melanogaster*. I. Mutations on the third chromosome. Genetics 122, 111-127.

Foe VE, Odell GM, Edgar BA (1993) Mitosis and Morphogenesis in the Drosophila Embryo: Point and Counterpoint. In The development of *Drosophila melanogaster* (ed. Bate, M., Arias, AM.), pp. 149-300. New York: Cold Spring Harbor Laboratory Press.

Grieder NC, de Cuevas M, Spradling AC (2000) The fusome organizes the MT network during oocyte differentiation in Drosophila. Development 127, 4253-4264.

Hari M, Wang Y, Veeraraghavan S, Cabral F (2003) Mutations in alpha- and beta-tubulin that stabilize MTs and confer resistance to colcemid and vinblastine. Mol Cancer Ther. 2, 597-605.

Heuer JG, Li K, Kaufman TC (1995) The Drosophila homeotic target gene centrosomin (cnn) encodes a novel centrosomal protein with leucine zippers and maps to a genomic region required for midgut morphogenesis. Development 121, 3861-3876.

Hutchens JA, Hoyle HD, Turner FR, Raff EC (1997) Structurally similar Drosophila alpha-tubulins are functionally distinct *in vivo*. Mol Biol Cell. 8, 481-500.

Janning W (1978) Gynandromorph fate maps in Drosophila. Results Probl. Cell Differ. 9, 1-28.

Ji JY, Squirrell JM and Schubiger G (2004) Both cyclin B levels and DNA-replication checkpoint control the early embryonic mitoses in Drosophila. Development 131, 401-411.

Kalfayan L, Wensink PC (1981) alpha-Tubulin genes of Drosophila. Cell. 24, 97-106.

Kamath K, Wilson L, Cabral F, Jordan MA (2005) BetaIII-tubulin induces paclitaxel resistance in association with reduced effects on MT dynamic instability. J Biol Chem. 13, 12902-12907.

Kwon M, Scholey JM (2004) Spindle mechanics and dynamics during mitosis in Drosophila. Trends Cell Biol. 14,194-205. Review. Erratum in: Trends Cell Biol. 14, 341-342.

Lee T, Luo L (1999) Mosaic analysis with a repressible neurotechnique cell marker for studies of gene function in neuronal morphogenesis. Neuron 22, 451-461.

Lewis SA, Gu W, Cowan NJ (1987) Free intermingling of mammalian beta-tubulin isotypes among functionally distinct MTs. Cell 49, 539-548.

Lindsley DL, Zimm GG (1992) The Genome of *Drosophila Melanogaster*. Academic Press, San Diego

Lowe J, Li H, Downing KH, Nogales E (2001) Refined structure of alpha beta-tubulin at 3.5 A resolution. J Mol Biol. 313, 1045-1057.

Luduena RF (1998) Multiple forms of tubulin: different gene products and covalent modifications. Int Rev Cytol. 178, 207-275.

Luo L, Liao YJ, Jan LY and Jan YN (1994) Distinct morphogenetic functions of similar small GTPases: Drosophila Drac1 is involved in axonal outgrowth and myoblast fusion. Genes Dev. 8, 1787-1802.

Mallik R and Gross SP (2004) Molecular motors: strategies to get along. Curr Biol. 14, 971-982.

Máthé E, Boros I, Jósvay K, Li K, Puro J, Kaufman TC, Szabad J (1998) The Tomaj mutant alleles of alpha Tubulin67C reveal a requirement for the encoded maternal specific tubulin isoform in the sperm aster, the cleavage spindle apparatus and neurogenesis during embryonic development in Drosophila. J Cell Sci 111, 887-896.

Matthews KA, Miller DF and Kaufman TC (1989) Developmental distribution of RNA and protein products of the Drosophila alpha-tubulin gene family. Dev. Biol. 132, 45-61.

Matthews KA, Rees D, Kaufman TC (1993) A functionally specialized alpha-tubulin is required for oocyte meiosis and cleavage mitoses in Drosophila. Development 3, 977-991.

Matthies HJ, Messina LG, Namba R, Greer KJ, Walker MY, Hawley RS (1999) Mutations in the alpha-tubulin 67C gene specifically impair achiasmate segregation in *Drosophila melanogaster*. J Cell Biol. 147, 1137-1144.

Menendez M, Rivas G, Diaz JF, Andreu JM (1998) Control of the structural stability of the tubulin dimer by one high affinity bound magnesium ion at nucleotide N-site. J. Biol. Chem. 273, 167-176.

Mischke D, Pardue ML (1982) Organization and expression of alpha-tubulin genes in *Drosophila melanogaster*. One member of the alpha-tubulin multigene family is transcribed in both oogenesis and later embryonic development. J. Mol. Biol. 156, 449-466.

Mitchison T, Kirschner M (1984) Dynamic instability of MT growth. Nature 312, 237–242.

Moore A, Wordeman L (2004) The mechanism, function and regulation of depolymerizing kinesins during mitosis. Trends Cell Biol. 14, 537-546.

Nogales E (1999) A structural view of MT dynamics. Cell Mol. Life Sci. 56, 133-142.

Reinsch S, Gonczy P (1998) Mechanisms of nuclear positioning. J. Cell Sci. 111, 2283-95.

Robinson JT, Wojcik EJ, Sanders MA, Mc Grail M, Hays TS (1999) Cytoplasmic dynein is required for the nuclear attachment and migration of centrosomes during mitosis in Drosophila. J. Cell Biol. 146, 597-608.

Schief WR, Clark RH, Crevenna AH, Howard J (2004) Inhibition of kinesin motility by ADP and phosphate supports a hand-over-hand mechanism. Proc. Natl. Acad. Sci. USA 101, 1183-1188.

Scholey, J. M, Brust-Mascher I, Mogilner A (2003) Cell division. Nature 422, 746-751.

Sharp DJ, Yu KR, Sisson JC, Sullivan W, Scholey JM (1999) Antagonistic MT-sliding motors position mitotic centrosomes in Drosophila early embryos. Nat. Cell Biol. 1, 51-54.

Sharp DJ, Brown HM, Kwon M, Rogewrs GC, Holland G, Scholey JM (2000a) Functional coordination of three mitotic motors in Drosophila embryos. Mol. Biol. Cell, 11, 241-253.

Sharp DJ, Rogers GC, Holland G, Scholey JM (2000b) MT motors in mitosis. Nature 407, 41-47.

Smith DE, Fisher PA (1984) Identification, developmental regulation, and response to heat shock of two antigenically related forms of a major nuclear envelope protein in Drosophila embryos: application of an

improved method for affinity purification of antibodies using polypeptides immobilized on nitrocellulose blots. J. Cell Biol. 99, 20-28.

Sullivan KF (1988) Structure and utilization of tubulin isotypes. Annu Rev Cell Biol. 4, 687-716.

Szabad J, Erdélyi M, Hoffmann G, Szidonya J, Wright TRF (1989) Isolation and characterization of dominant female sterile mutations of *Drosophila melanogaster*. II. Mutations on the second chromosome. Genetics 122, 823-835.

Scholey JM, Brust-Mascher I, Mogilner A (2003) Cell division. Nature 422, 746-751.

Sharp DJ, Yu KR, Sisson JC, Sullivan W, Scholey JM (1999) Antagonistic MT-sliding motors position mitotic centrosomes in Drosophila early embryos. Nat Cell Biol 1, 51-54.

Sullivan W, Theurkauf WE (1995) The cytoskeleton and morphogenesis of the early Drosophila embryo. Curr. Opin. Cell Biol. 7, 18-22.

Tadros W and Lipshitz HD (2005) Setting the stage for development: mRNA translation and stability during oocyte maturation and egg activation in Drosophila. Dev. Dyn. 232, 593-608.

Theurkauf WE (1992) Behavior of structurally divergent alpha-tubulin isotypes during Drosophila embryogenesis: evidence for post-translational regulation of isotype abundance. Dev. Biol. 154, 205-217.

Theurkauf WE, Baum H, Bo J, Wensink PC (1986) Tissue-specific and constitutive alpha-tubulin genes of *Drosophila melanogaster* code for structurally distinct proteins. Proc Natl Acad Sci U S A. 83, 8477-8481.

Tirian L, Puro J, Erdélyi M, Boros I, Papp B, Lippai M, Szabad J (2000) The Ketel(D) dominant-negative mutations identify maternal function of the Drosophila importin-beta gene required for cleavage nuclei formation. Genetics 156, 1901-1912.

Venkei Z., Szabad J. (2005) The *Kavar*^{D} dominant female-sterile mutations of Drosophila reveal role of the maternally provided α-tubulin^{4} isoform in cleavage spindle maintenance and elongation. Molecular Genetics and Genomics 273, 283-289.

Venkei Z., Gáspár I., Tóth G., Szabad J. (2006) α-tubulin^{4} is essential for rapid formation of lengthy interpolar MTs to push apart the daughter centrosomes along the nuclear perimeter during early Drosophila embryogenesis. J Cell Science, accepted for publication.

Wright AJ, Hunter CP (2003) Mutations in a beta-tubulin disrupt spindle orientation and MT dynamics in the early Caenorhabditis elegans embryo. Mol Biol Cell. 11, 4512-4525.

Wieschaus E, Nüsslein-Volhard C (1986) Looking at embryos. In: Roberts DB (ed) Drosophila, A Practical Approach. IRL Press, Oxford, pp. 199–228.

SUMMARY

The *Kavar*^{D} dominant-negative female-sterile mutations and their revertant *kavar*^{r} alleles identify the *αTub67C* gene of *Drosophila melanogaster*, which codes for the so-called maternal α-tubulin^{4} isotype. Although there is plenty of α-tubulin in every Drosophila egg yet in absence of α-tubulin^{4} (in eggs of the *kavar*^{null}/– females) only a tassel of short MTs forms nucleated by two barely separated daughter centrosomes and thus females without functional α-tubulin^{4}-coding *αTub67C* gene are sterile: α-tubulin^{4} is needed for the formation of lengthy MTs. Long MTs have been known (i) to form the prominent sperm aster to provide route for shipment of the female pronucleus into vicinity of the male pronucleus, (ii) to participate in formation of the embryonic nervous system and, as we described, (iii) in composing the interpolar MTs to push apart the daughter centrosomes along the nuclear perimeter during early Drosophila embryogenesis. Along with its newly discovered function, α-tubulin^{4} is enriched in the lengthy interpolar MTs that embrace the nuclear envelope. *In vitro* tubulin polymerization assays showed, that α-tubulin^{4} is required for rapid formation of long MTs. Since there is a time limit (set by the Cyclin-B/Cdk1 system) for MT formation during early embryogenesis, only short MTs form in absence of α-tubulin^{4}.

A tassel of short and straight MTs forms in every egg of the *Kavar*^{18c}/+ females whose egg cytoplasm contains E82K-α-tubulin^{4} besides normal α-tubulin^{4}. As confocal microscopy and *in vitro* polymerization assays showed the E82K-α-tubulin^{4} molecules are incorporated into the MTs, however they prevent the formation of lengthy MTs. The 82nd glutamic acid (E82) is involved in binding - through a Mg^{2+} - GTP, a structural component of the α-tubulins. Replacement of E82 by lysine (E82K) leads to MT instability. When injected into wild type early cleavage embryos traces of the E82K-α-tubulin^{4} containing cytoplasm kill the embryos through slowing down lengthy MT formation and separation of the daughter centrosomes. Remarkably, E82K-α-tubulin^{4} has no effect on late cleavage embryos in which the cleavage nuclei are only few micrometers apart in the egg cortex. When ectopically expressed (by the Gal4; UAS system) the E82K-α-tubulin^{4} molecules are incorporated into the MTs, however those can grow and function normally. It appears that α-tubulin^{4} was “designed” for the suitable rapid formation of MTs to reach over large distances in the early embryo.

ACKNOWLEDGMENTS

I wish to thank my scientific supervisor Professor János Szabad for his encouragement, guidance and support throughout my Ph.D. studies. The joint experimental work and the thought-provoking scientific discussions with dr. Imre Gáspár were of great pleasure. I wish to thank members of the Drosophila group at our department: dr. Mónika Lippai, Zsuzsa Sarkadi, dr. Miklós Erdélyi, dr. László Tirián, dr. Gyula Timinszky, dr. István Belecz, Balázs Ördög, dr. Péter Deák and Tamás Szalontai for their help, scientific conversations and comments. I am grateful for the technical support of Gabriella Teleki, Kissné Ani, dr. Kisapátiné Margó, Révész Kati, Piroska "néni" and Lajos "bácsi". My deepest thanks are dedicated to my parents, my girlfriend and my brother. They provided spiritual support all along the long time period of my Ph.D. studies.

We thank the generous help of Thomas C. Kaufman for the CNN antibody, Steffi Kuhfittig for *Df(3L)55*, Kathy Matthews for the *αTub67C*$^{-}$ alleles, Thomas Rudolph for the Drosophila genomic λ library, and Allan Spradling for the GFP:α-tubulin^{1} expressing line. Support for the above work came from the following sources. (1) Hungarian Academy of Sciences, Maternal-Effect and Embryogenesis Research Group. (2) An FKFP Grant (No. 1348). (3) Graduate Student Program of the University of Szeged.